



## Increasing glutathione levels by a novel posttranslational mechanism inhibits neuronal hyperexcitability

Ashwini Sri Hari<sup>a</sup>, Rajeswari Banerji<sup>a</sup>, Li-Ping Liang<sup>a</sup>, Ruth E. Fulton<sup>a</sup>, Christopher Quoc Huynh<sup>a</sup>, Timothy Fabisiak<sup>a</sup>, Pallavi Bhuyan McElroy<sup>b</sup>, James R. Roede<sup>a</sup>, Manisha Patel<sup>a,\*</sup>

<sup>a</sup> Department of Pharmaceutical Sciences, University of Colorado, Anschutz Medical Campus, Aurora, CO, 80045, USA

<sup>b</sup> The Janssen Pharmaceutical Companies of Johnson & Johnson, Greater Philadelphia Area, Horsham, PA, 19044, USA

### ARTICLE INFO

#### Keywords:

Oxidative stress  
Neuronal hyperexcitability  
Glutamate cysteine ligase  
Glutathione  
mTORC1

### ABSTRACT

Glutathione (GSH) depletion, and impaired redox homeostasis have been observed in experimental animal models and patients with epilepsy. Pleiotropic strategies that elevate GSH levels *via* transcriptional regulation have been shown to significantly decrease oxidative stress and seizure frequency, increase seizure threshold, and rescue certain cognitive deficits. Whether elevation of GSH *per se* alters neuronal hyperexcitability remains unanswered. We previously showed that thiols such as dimercaprol (DMP) elevate GSH *via* post-translational activation of glutamate cysteine ligase (GCL), the rate limiting GSH biosynthetic enzyme. Here, we asked if elevation of cellular GSH by DMP altered neuronal hyperexcitability *in-vitro* and *in-vivo*. Treatment of primary neuronal-glia cerebral cortical cultures with DMP elevated GSH and inhibited a voltage-gated potassium channel blocker (4-aminopyridine, 4AP) induced neuronal hyperexcitability. DMP increased GSH in wildtype (WT) zebrafish larvae and significantly attenuated convulsant pentylenetetrazol (PTZ)-induced acute 'seizure-like' swim behavior. DMP treatment increased GSH and inhibited convulsive, spontaneous 'seizure-like' swim behavior in the Dravet Syndrome (DS) zebrafish larvae (*scn1Lab*). Furthermore, DMP treatment significantly decreased spontaneous electrographic seizures and associated seizure parameters in *scn1Lab* zebrafish larvae. We investigated the role of the redox-sensitive mammalian target of rapamycin (mTOR) pathway due to the presence of several cysteine-rich proteins and their involvement in regulating neuronal excitability. Treatment of primary neuronal-glia cerebral cortical cultures with 4AP or L-buthionine-(S,R)-sulfoximine (BSO), an irreversible inhibitor of GSH biosynthesis, significantly increased mTOR complex I (mTORC1) activity which was rescued by pre-treatment with DMP. Furthermore, BSO-mediated GSH depletion oxidatively modified the tuberous sclerosis protein complex (TSC) consisting of hamartin (TSC1), tuberin (TSC2), and TBC1 domain family member 7 (TBC1D7) which are critical negative regulators of mTORC1. In summary, our results suggest that DMP-mediated GSH elevation by a novel post-translational mechanism can inhibit neuronal hyperexcitability both *in-vitro* and *in-vivo* and a plausible link is the redox sensitive mTORC1 pathway.

### 1. Introduction

Over 65 million people globally suffer from epilepsy, an 'energy-expensive' neurological disorder characterized by recurrent, spontaneous seizures. Regardless of its etiology [1,2], key cellular, molecular, and circuit-level alterations are observed in the epileptic brain. Despite the availability of several antiseizure drugs, ~33% of the epilepsy population exhibit pharmacoresistance [3,4]. This could be attributed to

symptomatic relief offered by current medications rather than targeting underlying disease mechanisms. Given the complexity of mechanisms involved in seizure generation and epilepsy development [5,6], there is an urgent, unmet medical need for the development of treatment strategies that target such mechanisms to offer adequate seizure control.

Acute and chronic seizure activity are known to result in increased steady-state levels of reactive species (RS) production from various cellular sources, especially from the mitochondria, and nicotinamide adenine dinucleotide phosphate reduced (NADPH) oxidase systems

\* Corresponding author. Department of Pharmaceutical Sciences, University of Colorado Anschutz Medical Campus, 12850 E. Montview Blvd, Aurora, CO, 80045, USA.

E-mail address: [Manisha.Patel@cuanschutz.edu](mailto:Manisha.Patel@cuanschutz.edu) (M. Patel).

<https://doi.org/10.1016/j.redox.2023.102895>

Received 21 August 2023; Received in revised form 14 September 2023; Accepted 18 September 2023

Available online 21 September 2023

2213-2317/© 2023 Published by Elsevier B.V. This is an open access article under the CC BY-NC-ND license (<http://creativecommons.org/licenses/by-nc-nd/4.0/>).

Abbreviations	
%	Percent
~	Approximately
3 MP	3-mercapto-1-propanol
4AP	4-aminopyridine
AxIS	Axion Integrated Software
BCA	Bicinchoninic acid
BME	$\beta$ -mercaptoethanol
BSA	Bovine serum albumin
BSO	L-buthionine-(S,R)-sulfoximine
Ca <sup>2+</sup>	Divalent calcium
DIV	Days <i>in-vitro</i>
DMF	Dimethyl fumarate
DMP	Dimercaprol
DMSO	Dimethyl sulfoxide
dpf	Days post fertilization
DS	Dravet Syndrome
DTT	Dithiothreitol
EC	Electrochemical detection
ECL	Enhanced chemiluminescence
EDTA	Ethylenediamine tetraacetic acid
FBS	Fetal bovine serum
GAP	GTPase activating protein
GCL	Glutamate cysteine ligase
GCLC	Glutamate cysteine ligase catalytic subunit
GCLM	Glutamate cysteine ligase modifier subunit
GMEM	Glucose and serum containing minimum essential media
Gpx	Glutathione peroxidase
Grx	Glutaredoxin
GSH	Reduced glutathione
GSSG	Oxidized glutathione
GST	Glutathione-S-transferase
GTP	Guanosine triphosphate
h	Hour
H <sub>2</sub> O <sub>2</sub>	Hydrogen peroxide
HBSS	Hank's balanced salt solution
HEPES	4-(2-hydroxyethyl)-1-piperazineethanesulfonic acid
HPLC	High performance liquid chromatography
HRP	Horseradish peroxidase
HS	Horse serum
K <sup>+</sup>	Potassium ion
KD	Ketogenic diet
kDa	Kilodalton
LDH	Lactate dehydrogenase
LMA	Low melting agarose
LFP	Local field potential
MEA	Microelectrode array
MEM	Minimum essential media
mg/mL	Milligrams/milliliter
min	Minutes
mm/s	Millimeter/second
mM	Millimolar
mPEG	Maleimide-polyethylene glycol
ms	Millisecond
mTOR	Mammalian (mechanistic) target of rapamycin
mTORC1	mTOR complex I
mTORC2	mTOR complex II
N	Normal (as in normality)
NAC	N-acetyl cysteine
NADH	Nicotinamide adenine dinucleotide reduced
NADPH	Nicotinamide adenine dinucleotide phosphate reduced
NEM	N-ethylmaleimide
Nrf2	Nuclear factor erythroid 2-related factor 2
O <sub>2</sub> <sup>-</sup>	Superoxide anion
OXPPOS	Oxidative phosphorylation
PCA	Perchloric acid
<i>pck1</i>	Gene encoding phosphoenolpyruvate carboxykinase 1
PDL	Poly-D-lysine
PEDOT	Poly(3,4-ethylenedioxythiophene) polystyrene sulfonate
PEG	Polyethylene glycol
PI3K	Phosphoinositide-3-kinase
PKB or Akt	Protein kinase B
PTZ	Pentylenetetrazol
PVDF	Polyvinylidene difluoride
Rheb	Ras homolog enriched in brain
RNS	Reactive nitrogen species
ROS	Reactive oxygen species
rpm	Revolutions per minute
RS	Reactive species
RT	Room temperature
S6	Ribosomal protein S6
S6K	Ribosomal protein S6 kinase
SCN1A	Gene encoding voltage-gated sodium channel subunit $\alpha$
<i>scn1Lab</i>	Dravet Syndrome mutant/zebrafish larvae
SDS	Sodium dodecyl sulfate
SE	<i>Status epilepticus</i>
SFN	Sulforaphane
SLE	Systemic lupus erythematosus
SMEI	Severe Myoclonic Epilepsy of Infancy
SUDEP	Sudden unexpected death in epilepsy
T cells	T lymphocytes
TBC1D7	TBC1 domain family member 7
TBS	Tris buffered saline
TBS-T	Tris buffered saline with 0.1% tween-20
TCA cycle	Tricarboxylic acid cycle
TCEP	Tris (2-carboxyethyl) phosphine hydrochloride
TL	Tüpfel long fin
t-S6	Total ribosomal protein S6
TSC	Tuberous sclerosis protein complex
TSC1	Tuberous sclerosis protein 1 (hamartin)
TSC2	Tuberous sclerosis protein 2 (tuberin)
Veh ctrl	Vehicle control
vs	Versus
$\beta$ -Tubulin or B-Tubulin	Beta tubulin
$\mu$ m	Micrometer
$\mu$ M	Micromolar

[7–10]. Failure to detoxify seizure-induced excess RS is known to further perpetuate seizures [11,12]. Persistent increases in steady-state levels of RS can significantly alter the cellular redox tone which can lead to impaired antioxidant defenses, dysfunction of redox circuitry in signal transduction pathways, altered neuroinflammatory responses, oxidative damage, and eventually the death of vulnerable neurons.

Chronically depleted glutathione (GSH) levels and an impaired GSH redox status have been observed in several experimental animal models

of epilepsy [9,10,13,14] and epilepsy patients [15]. GSH is a tripeptide (glutamate, cysteine, and glycine) and the most abundant non-protein antioxidant thiol found in millimolar (~2 mM) concentrations in the brain [16]. The GSH antioxidant system is a critical redox buffer that maintains redox homeostasis by detoxifying hydrogen peroxide (H<sub>2</sub>O<sub>2</sub>) and is critical in the brain due to its limited antioxidant capacity, the presence of transition metals like iron, and high unsaturated lipid content [17–19]. GSH redox homeostasis is essential for the activity of

GSH-dependent antioxidant enzymes such as glutathione peroxidases (GPx), transferases (GST), and glutaredoxins (Grx). Treatment strategies that increase GSH levels significantly decreased oxidative stress, and pro-inflammatory mediator release, reduced frequency of spontaneous seizures and rescued certain cognitive deficits [20–25]. However, how GSH elevation attenuates neuronal hyperexcitability and neuro-inflammation is incompletely understood. Current metabolic therapeutic strategies known to increase GSH such as the ketogenic diet (KD), GSH precursors like N-acetyl cysteine (NAC), nuclear factor erythroid 2-related factor 2 (Nrf2) inducers such as dimethyl fumarate (DMF), sulforaphane (SFN) rely on Nrf2 transcriptional upregulation to increase GSH levels. However, Nrf2 upregulation can be pleiotropic, and Nrf2 induction may fail in the injured and aging brain given the increased expression of its transcriptional repressors [26,27]. Hence, there is an unmet need to develop drugs that can increase GSH levels by novel mechanisms.

Dimercaprol (DMP) is a dithiol compound that is approved for human use to treat heavy metal poisoning [28]. A previous study from our laboratory demonstrated that DMP can increase intracellular GSH levels by a novel mechanism: post-translational activation of the biosynthetic enzyme, GCL (glutamate cysteine ligase). GCL is composed of two subunits: catalytic (GCLC) and modifier (GCLM) subunits and is the rate-limiting enzyme in GSH biosynthesis. DMP increases GCL holoenzyme formation and activity in different cell types and attenuates pro-inflammatory mediator release [21]. This novel approach to elevate *de novo* synthesis of GSH could overcome caveats associated with transcriptional Nrf2 upregulation.

How redox status controls neuronal excitability remains an enigma. A common mechanism is thiol modification of seizure-inducing cell signaling pathways. One such pathway, the mammalian (mechanistic) target of rapamycin (mTOR) pathway (consisting of mTOR complexes I and II (mTORC1 and mTORC2)) is known to be redox-sensitive and controls neurotransmission, ion channel formation, and synaptic plasticity [29–31]. Aberrantly activated mTORC1 and in some cases, mTORC2 [32] have been observed in many chemoconvulsant-induced [32–38] and genetic models [39–42] of uncontrolled seizure activity. Interestingly, mTOR inhibitors such as rapamycin and its analogs that allosterically inhibit mTORC1 predominantly [43,44] have shown to decrease seizure activity [45–47]. However, the discontinuation of mTOR inhibitors can lead to seizure reemergence in several cases [48] thereby necessitating the identification of new strategies to regulate mTOR activity. Evidence from literature suggests that oxidative stress can hyperactivate mTORC1 [49] and oxidatively modify critical proteins in this pathway. The tuberous sclerosis protein complex (TSC) comprising TSC1, TSC2, and TBC1D7 [50] is a critical upstream negative regulator of mTORC1. TSC1 and TBC1D7 together provide stability for TSC2 and prevent its degradation by ubiquitination [50,51]. The structural stability of TSC2 is critical to exert its guanosine triphosphate (GTP)ase activating protein (GAP) activity towards a small Ras family GTPase called Ras homolog enriched in brain (Rheb) [52,53] which is essential for the inhibition of downstream mTORC1 kinase activity [54, 55]. The TSC proteins have several key cysteine residues (rat TSC1 (~18); rat TSC2 (~41); rat TBC1D7 (~8)) that are susceptible to cellular redox modulations. Studies from literature show that cysteine oxidants hyperactivate and reducing agents dampen mTORC1 activity by acting mainly through the TSC protein complex [56,57]. The aberrant activation of mTORC1 and GSH depletion occur concomitantly in several acquired and some genetic epilepsy models [33,34,38,41], however, whether GSH redox status modulates mTORC1 activity is largely unknown.

In this study, we asked if GSH elevation by DMP attenuated 4-aminopyridine (4AP)-induced neuronal hyperexcitability in primary neuronal-glial cerebrocortical cultures *in-vitro* and in a zebrafish model of epilepsy. Furthermore, we examined proteins essential in the mTOR pathway to link redox sensitivity with hyperexcitability. The results indicate that the modulation of GCL using either L-buthionine-(S,R)-

sulfoximine (BSO, an irreversible inhibitor of GCL) or DMP (post-translational activator of GCL) alters mTORC1 signaling *in-vitro*. We also show that GSH depletion oxidatively modifies TSC1, TSC2, and TBC1D7 in the TSC protein complex. Finally, we show that DMP elevates GSH levels *in-vivo* in two different larval zebrafish models. DMP elevates GSH and attenuates pentylenetetrazol (PTZ)-induced acute ‘seizure-like’ swim behavior in wildtype (WT) larvae. Additionally, we show that DMP increases GSH levels and attenuates spontaneous ‘seizure-like’ swim behavior and electrographic seizures in *scn1Lab* (Dravet Syndrome (DS)) larval zebrafish mutants with chronic epilepsy.

## 2. Experimental procedures

### 2.1. Chemical reagents

All chemicals and reagents were obtained from Sigma-Aldrich (St. Louis, MO, USA) unless otherwise noted.

### 2.2. Cell culture

All cell culture reagents were purchased from Invitrogen. Mixed primary neuronal-glial cerebrocortical cultures were prepared using the protocol as described previously [58] and modified. Briefly, cerebral cortices from embryonic day 18 (E18) rat pups were dissected and enzymatically dissociated by incubation in Ca<sup>2+</sup>- and Mg<sup>2+</sup>-free Hank's balanced salt solution (HBSS) supplemented with 10 mM 4-(2-hydroxyethyl)-1-piperazineethanesulfonic acid (HEPES) and 0.25% trypsin for 25min at 37 °C. The tissue was rinsed and dispersed into a single-cell suspension using a fire-polished Pasteur pipette. The cell suspension was centrifuged and resuspended in minimum essential media (MEM) containing Earle's salts supplemented with 3 g/L glucose, 5% horse serum (HS), and 5% fetal bovine serum (FBS). The cells were plated at an initial density of 1.5 \* 10<sup>6</sup> cells/well on poly-D-lysine (PDL) coated 6-well plates for reduced glutathione/oxidized glutathione (GSH/GSSG) assay, and immunoblotting, 1.5\* 10<sup>5</sup> cells/well on PDL coated 96-well plates for the cytotoxicity assay, and 3.0 \* 10<sup>4</sup> cells/well on PDL coated 48-well plates for microelectrode array (MEA) assay and maintained at 37 °C in a humidified incubator with 5% CO<sub>2</sub>/95% air in growth medium. Mature cells were used at 14–16 days *in-vitro* (DIV) for all experiments. All experiments were conducted in serum-free MEM media unless otherwise noted.

All cell culture experiments were replicated for a minimum of 3 times (3 independent experiments). For each experiment, primary neuronal-glial cerebrocortical cultures were prepared from embryonic D18 rat pups obtained from a pregnant rat dam. The ‘n’ in the figure legends associated with cell culture experiments represents the number of technical replicates per treatment condition per experimental run and, ‘N’ represents the number of experimental replicates i.e. pregnant dams.

### 2.3. Neuronal hyperexcitability measurement by MEA

Neuronal spiking/excitability was measured on 48-well Classic MEA plates. Each well contains an array of 16 embedded gold electrodes for a total of 768 low noise recording electrodes (Axion Biosystems INC, Atlanta, GA, USA). Primary neuronal-glial cerebrocortical cultures were plated on PDL coated MEA plates at an initial density of 3.0\*10<sup>4</sup> cells/well in 500 µL/well of glucose-containing MEM media. On the day of the experiment, cells were acclimated in 250 µL of serum-free MEM media/well for 1 h before drug treatment. All drugs were prepared in serum-free MEM. After treatment with DMP (or other thiol-containing compounds) for 4 h, cultures were stimulated with 4AP for 1 h. Spontaneous network activity was recorded by Axion's Integrated Studio (AxIS 2.1.1) software with neural real-time-spontaneous recording settings. Neuronal activity was recorded every 15 min for a 2-min epoch for a total of 1 h after 4AP stimulation. Any wells that did not show spontaneous activity on the day of the experiment were excluded from the

study. For data analysis, any wells that had less than five active electrodes/well in the baseline recording were excluded from the study. Extracellular action potential recordings were represented as number of spikes.

#### 2.4. High-performance liquid chromatography (HPLC) measurement of GSH and GSSG levels

Primary neuronal-glia cerebrocortical cultures were seeded at an initial density of  $1.5 \times 10^6$  cells/well in 6-well plates coated with PDL. On 14DIV, cultures were acclimated for 1 h in serum-free MEM, treated, collected after the appropriate time-point, and stored at  $-80^\circ\text{C}$ . GSH and GSSG were measured with an ESA 5600 CoulArray HPLC system (Chelmsford, MA, USA) on two coulometric array cell modules, each containing four electrochemical sensors attached in series as previously described before [59]. The potentials of the electrochemical cells were set at 150/300/450/580/700/820 mV versus palladium (Pd). Frozen cell samples were sonicated at 31% amplitude (Fisher Scientific Sonic Dismembrator 500, Waltham, MA, USA) in 200  $\mu\text{L}$  of cold 0.1 N perchloric acid (PCA) prior to thawing. The homogenates were then centrifuged at 13,000 revolutions per minute (rpm) for 10 min at  $4^\circ\text{C}$ . A 150  $\mu\text{L}$  aliquot of the supernatant from each sample was injected into the HPLC and analytes were separated on a 150x4.6 mm C-18 reverse phase YMC ODS-A column (Waters Co., Milford, MA, USA) (5  $\mu\text{m}$  particle size). The mobile phase was composed of 100 mM monobasic sodium phosphate ( $\text{NaH}_2\text{PO}_4$ ) and 1% methanol, pH 3.0, with a flow rate of 0.6 mL/min. The pellet was dissolved in 200  $\mu\text{L}$  of 0.05 N sodium hydroxide (NaOH), sonicated at 31% amplitude, and used to determine sample protein concentration by the Bradford protein assay. GSH and GSSG values were normalized to cellular protein concentrations. Total glutathione values were calculated using the formula:  $[\text{GSH} + (2 \times \text{GSSG})]$  after GSH and GSSG values were normalized to protein concentration.

#### 2.5. Western blotting

Primary neuronal-glia cerebrocortical cultures were seeded at an initial density of  $1.5 \times 10^6$  cells/well on 6-well plates coated with PDL. On 14DIV, cultures were acclimated for 1 h in serum-free MEM, treated, collected after the appropriate time-point, and stored at  $-80^\circ\text{C}$ . For processing samples, cell pellets were solubilized by sonication (31% amplitude, Fisher Scientific Sonic Dismembrator 500, Waltham, MA, USA) in 100  $\mu\text{L}$  lysis buffer made up of 1X phosphate buffered saline (PBS), 1 protease inhibitor tablet (Roche complete mini, Basel, Switzerland), 100  $\mu\text{L}$  phosphatase inhibitor (Sigma, St. Louis, MO, USA). Sonicated samples were centrifuged at 13,000 rpm for 10 min at  $4^\circ\text{C}$ . Protein estimation was done by the Bradford protein assay. Samples (10–15  $\mu\text{g}$  protein) prepared in 1X PBS were mixed with 2X Laemmli buffer (Bio-Rad, Hercules, CA, USA) containing 5%  $\beta$ -mercaptoethanol (BME) and boiled for 10 min at  $95^\circ\text{C}$  on a heat block. 15  $\mu\text{L}$  of samples were run on 4–20% gradient sodium dodecyl sulfate (SDS) gels (Bio-Rad) at 200V for 35–40 min. Proteins were transferred onto polyvinylidene difluoride (PVDF) membranes using a Trans-Blot Turbo™ semi-dry transfer system (Bio-Rad), blocked with 5% bovine serum albumin (BSA, Sigma, MO, USA), and probed with the phospho-S6 ribosomal protein [60–62] (1:1000, 32 kDa), and  $\beta$ -tubulin [63–65] (1:1000, 55 kDa) rabbit primary antibodies.  $\beta$ -tubulin was used as a loading control to ensure effective protein transfer and equal sample loading across all wells. For detecting total-S6 ribosomal protein, the same blot was stripped using the Restore™ PLUS Western blot stripping buffer (Thermo Fisher Scientific, Waltham, MA, USA) for ~8 min, washed with 1X tris buffered saline (TBS), blocked for 1 h with 5% BSA, and then probed using the total S6 ribosomal protein [66–68] rabbit primary antibody (1:1000, 32 kDa). All antibodies were purchased from Cell Signaling Technology (Danvers, MA, USA). Precision Plus protein Kaleidoscope ladder (Bio-Rad) was used. Membranes were probed with horseradish peroxidase (HRP)-conjugated goat anti-rabbit secondary

antibody (Abcam, Cambridge, MA), at a dilution of 1:10,000 in TBS containing 0.1% tween-20 (TBS-T). Membranes were developed using the SuperSignal™ West Pico PLUS enhanced chemiluminescence (ECL) reagent (Thermo Fisher Scientific, Waltham, MA, USA) and protein levels were visualized and quantified using the Gel-Doc system and Image Lab 5.0 software (Bio-Rad). mTORC1 activity was quantified by assessing the phospho (p-S6) to total (t-S6) S6 ribosomal protein ratio.

#### 2.6. Cell injury assessment

Primary neuronal-glia cerebrocortical cultures were seeded in 96-well plates coated with PDL at an initial density of  $1.5 \times 10^5$  cells/well. On 14DIV, cells were acclimated for 1 h in serum-free MEM, treated for 24 h with drug compounds, and media was collected for an lactate dehydrogenase (LDH) release assay. LDH activity was measured in media as described previously [69]. Briefly, 20  $\mu\text{L}$  of media from drug-treated wells was transferred into a new 96-well plate. To this, 20  $\mu\text{L}$  of 1.6 mM pyruvate and 110  $\mu\text{L}$  of 0.2 mM nicotinamide adenine dinucleotide reduced (NADH) solutions prepared in Tris/NaCl buffer were added at room temperature (RT) and kinetics of the enzymatic reaction were immediately measured using a spectrophotometer (Molecular Devices, Spectramax, San Jose, CA, USA). LDH activity was measured spectrophotometrically at  $30^\circ\text{C}$  as the amount of pyruvate consumed, by monitoring the decrease in absorbance because of NADH oxidation at 340 nm.

#### 2.7. Redox western blotting

Primary neuronal-glia cerebrocortical cultures were seeded at an initial density of  $1.5 \times 10^6$  cells/well in 6-well plates coated with PDL. On 14 DIV, cultures were acclimated for 1 h in serum-free MEM, treated, and collected in N-ethylmaleimide (NEM) to preserve/protect redox-states of thiols in the sample. Briefly, cultures were washed with 1X PBS once after treatment, followed by the addition of 100  $\mu\text{L}$  of alkylating buffer containing 0.5 M HEPES, 0.5 M ethylenediamine tetraacetic acid (EDTA), 4 N sodium chloride (NaCl), and ~99.8  $\mu\text{M}$  NEM and incubation at RT for 15 min. Then, 10  $\mu\text{L}$  of 10% SDS was added, and cultures were collected and sonicated (31% amplitude, Fisher Scientific Sonic Dismembrator 500, Waltham, MA, USA) to reduce viscosity. Excess NEM was desalted using 2 mL spin-columns (Thermo Fisher Scientific, Waltham, MA, USA), and resulting protein concentrations were estimated by the bicinchoninic acid (BCA) protein assay. Samples (12–15  $\mu\text{g}$  protein) were prepared in 1X PBS buffer and underwent a series of thiol-based derivatization steps. Samples were incubated with 1  $\mu\text{L}$ /sample of 1 mM Tris (2-carboxyethyl) phosphine hydrochloride (TCEP) for 15 min at RT followed by desalting of excess TCEP by 0.5 mL protein desalting columns (Thermo Fisher Scientific, Waltham, MA, USA). Next, 2  $\mu\text{L}$ /sample of 0.6 mM of 2 k maleimide-polyethylene glycol (mPEG, Creative PEGWorks, Chapel Hill, NC, USA) was added to samples and incubated for 30 min at RT. Finally, to halt mPEG conjugation, 1  $\mu\text{L}$ /sample of 0.5 mM dithiothreitol (DTT) was added and incubated for 5 min at RT. 4X Laemmli buffer was added to samples (without BME). 30  $\mu\text{L}$  of samples were run (without boiling) on 7.5% stain-free gel (Bio-Rad) at 200V for 35–40 min. Proteins were transferred onto PVDF membranes using a Trans-Blot Turbo™ semi-dry transfer system (Bio-Rad), blocked with 5% BSA (Sigma, MO, USA), and probed with the total protein rabbit primary antibodies for TSC1 [70–72] (1:1000; 150–170 kDa), TSC2 [73–75] (1:1000; 200 kDa), TBC1D7 [76–78] (1:1000; 30 kDa).  $\beta$ -tubulin [63–65] (1:1000; 55 kDa) was used as a loading control. Total protein levels of TSC1, TSC2, and TBC1D7 were normalized to the loading control. All antibodies were purchased from Cell Signaling Technology (Danvers, MA, USA). Precision Plus protein Kaleidoscope ladder (Bio-Rad) was used. Membranes were probed with HRP-conjugated goat anti-rabbit secondary antibody (Abcam, Cambridge, MA) at a dilution of 1:10,000 in 1X TBS-T. Membranes were developed using the SuperSignal™ West Pico PLUS ECL reagent

(Thermo Fisher Scientific, Waltham, MA, USA) and protein levels were visualized and quantified using the Gel-Doc system and Image Lab 5.0 software (Bio-Rad). Oxidation of TSC1, TSC2, and TBC1D7 total proteins was quantified by assessing changes in their respective band intensities (normalized to  $\beta$ -tubulin) compared to vehicle control.

## 2.8. Statement on the ethical treatment of animals

Our studies were carried out in strict accordance with the recommendations in the Guide for the Care and Use of Laboratory Animals of the National Institutes of Health (NIH). All procedures were approved by the Institutional Animal Care and Use Committee (IACUC) of the University of Colorado Denver (UCD), which is fully accredited by the Association for Assessment and Accreditation of Laboratory Animal Care (AAALAC). All animal experiments complied with the ARRIVE guidelines and the National Research Council's Guide for the Care and Use of Laboratory Animals. All experiments were designed to minimize pain and discomfort and conform to NIH regulatory standards of care.

## 2.9. Zebrafish housing and husbandry

Zebrafish (*Danio rerio*) were maintained in the Animal Core Facility located at UCD according to standard procedures [79]. Zebrafish were housed in a temperature-controlled facility under the standard light/dark (14:10 h) cycle. The temperature was tightly regulated and varied from 27 °C to 29 °C [79]. Water quality was monitored automatically and dosed to maintain conductivity (1000–1050  $\mu$ S) and pH (6.95–7.30). The filtration system consisted of a bead filter, fluidized bed biofilter, finishing filters (bag filters), and UV sterilization. Zebrafish embryos were raised at 28.5 °C in embryo medium consisting of 0.03% Instant Ocean (Aquarium Systems, Inc., Mentor, OH, USA) in deionized water containing 0.2 ppm methylene blue as a fungicide [80]. Larvae were maintained in round Petri dishes (20 mm depth) in an incubator with a similar light-dark cycle. The housing density was limited to approximately 50 larvae per dish. Adult zebrafish were housed in 1.5 L tanks with a stock density of 5–10 fish/tank and fed twice daily with adult commercial zebrafish diet (Gemma 300).

## 2.10. Zebrafish lines

The zebrafish strains used in this study were Tüpfel long fin (TL) (WT) and homozygous mutants *scn1Lab*<sup>-/-</sup> (*didy*<sup>s552</sup>) (Dravet Syndrome, DS) maintained on a TL strain background [81]. The *scn1Lab*<sup>-/-</sup> larvae were obtained by crossing adult *scn1Lab*<sup>+/-</sup> zebrafish and were sorted by their unique dark pigmentation. All experiments were performed with 5–7 days post fertilization (dpf) larvae which were randomly selected as sex determination was not possible at the early stages [82]. One limitation of the *scn1Lab* mutant larvae that restricts long-term studies is that they have a shorter lifespan, and they die prematurely between 10 and 12 dpf [81,83]. For obtaining ~60–70 WT embryos, two to three tanks were set-up containing parental strains in the ratio of one male to two female adult zebrafish (TL)/tank. For obtaining more than 100 WT embryos, four to six tanks were set-up containing parental strains in the same ratio. One tank usually yields about 25–50 viable WT embryos which are then allowed to hatch in a 28.5 °C incubator. For obtaining ~60–70 DS embryos, five to seven tanks were set-up containing parental strains in the ratio of one male to two female adult zebrafish (*scn1Lab*<sup>+/-</sup>)/tank. For obtaining more than 100 DS embryos, six to nine tanks were set-up containing parental strains in the same ratio. From one clutch, only 25% of the embryos will be homozygous (*scn1Lab*<sup>-/-</sup>) DS mutants. All *in-vivo* experiments were replicated for a minimum of 3 times (3 independent experiments). The 'n' in the figure legends associated with *in-vivo* experiments represents the number of zebrafish larvae utilized per treatment condition per experimental run and, 'N' represents the number of experimental replicates.

## 2.11. HPLC assay for GSH and GSSG measurement in zebrafish larvae

The stock concentration of DMP (100 mM) was made in dimethyl sulfoxide (DMSO). Drug dilutions were made with embryo media and pH adjusted to 7–7.5 to prepare the working concentrations. Whole zebrafish larvae and not just larval brains were utilized for the HPLC assay for two reasons: (i) we first wanted to demonstrate that the small molecule DMP would work in a vertebrate model system (proof of concept), and (ii) given the limited yield of *scn1Lab* zebrafish larvae, pooling of larval brains for samples and associated replicates to achieve minimum levels of detection for GSH/GSSG in our HPLC system would be technically challenging. Wildtype (WT) and *scn1Lab* zebrafish larvae were treated (after 1 h acclimation) in a 6-well plate with different doses of DMP for 4 h in a 28.5 °C incubator with light/dark cycles. Approximately 50–70 larvae/group/sample were pooled for the GSH assay. The final concentration of DMSO for all drug dilutions was less than 1%. Post-treatment, every larva was checked under the microscope to rule out the possibility of poor health and drug toxicity based on three criteria: a) a visible beating heart; and b) movement in response to touch or external stimulus; and c) absence of physical deformities. A drug was considered toxic if no visible heartbeat or movement in response to touch or external stimulus was detected in at least 50% of the test larvae after the drug treatment period [81]. After treatment, larvae were collected and stored at –80 °C. For the HPLC assay, larvae were solubilized by sonication (34% amplitude) (Fisher Scientific Sonic Dismembrator 500, Waltham, MA, USA) in 200  $\mu$ L of cold 0.1 N PCA, centrifuged at 13,000 rpm for 10min at 4 °C. Samples were sonicated twice to ensure complete dissociation of larval tissue. 150  $\mu$ L of the supernatant from each sample was loaded onto the HPLC and analytes were separated on a 150x4.6 mm C-18 reverse phase YMC ODS-A column (Waters Com., Milford, MA, USA) (5  $\mu$ m particle size). The mobile phase was composed of 100 mM NaH<sub>2</sub>PO<sub>4</sub> and 1% methanol, pH 3.0, with a flow rate of 0.6 mL/min. The pellet was resuspended in 200  $\mu$ L of 0.05 N NaOH, sonicated at 34% amplitude, and used for protein estimation. GSH and GSSG values were normalized to cellular protein concentrations determined by the Bradford protein assay. Total glutathione values were estimated from GSH and GSSG values normalized to larval tissue protein concentrations.

## 2.12. Monitoring of larval swim behavior

For tracking zebrafish larval swim behavior, we followed an acute locomotion assay protocol using the DanioVision system running the EthoVision XT software (Noldus Information Technology, Leesburg, VA, USA) as established previously [81]. The Noldus DanioVision system is designed for high-throughput testing of zebrafish larvae in multi-well plates and has been used in studies related to drug screening/development (e.g., novel anticonvulsants), safety pharmacology, behavioral genetics, toxicology, and circadian rhythmicity. The observation chamber of the DanioVision system utilizes a high-quality camera for video-tracking locomotion, Fresnell lenses to prevent image distortion, a plate holder backlit with infra-red (IR) light (at a wavelength invisible to zebrafish larvae) to help with tracking larval movement in the dark, and a video-tracking algorithm (EthoVision XT) that can accurately track up to 100 subjects at a time [84]. Larval 'seizure-like' swim behavior was assessed by analyzing the locomotion plots obtained from the EthoVision XT software for mean velocity (mm/s) values. The treatment paradigm followed prior to assessing either acute, convulsant PTZ-induced 'seizure-like' swim behavior in WT larvae or spontaneous 'seizure-like' swim behavior in DS mutants was different. 5-7 dpf WT larvae were placed individually in a 96-well plate with 100  $\mu$ L embryo media in each well. The larvae were first acclimatized by placing them in the DanioVision chamber under dark light for a 20min period followed by a 10min baseline recording epoch. After obtaining baseline measurements, the embryo media was replaced with 100  $\mu$ L DMP (1, 10, 30, or 100  $\mu$ M) or DMSO (vehicle, <1%) in control wells and incubated for a

period of 4 h. After 4 h, certain groups of larvae were treated with 11.11  $\mu\text{L}$  of either 10 mM PTZ or embryo media for vehicle control for an additional 40min followed by a 10min recording epoch to assess acute 'seizure-like' swim behavior. For assessing spontaneous, convulsive 'seizure-like' swim behavior in DS mutants, 5-7dpf *scn1Lab* larvae were placed individually in 96-well plates with 100  $\mu\text{L}$  embryo media in each well. The larvae were first acclimatized by placing them in the DanioVision chamber under dark light for a 20min period followed by a 10min baseline recording epoch. After obtaining baseline measurements, the embryo media was replaced with 100  $\mu\text{L}$  DMP (10, 30, or 100  $\mu\text{M}$ ) or DMSO (vehicle, <1%) in control wells or stiripentol (10  $\mu\text{M}$ ) that was used as a positive control and incubated for a period of 4 h. The treatment period was followed by a 10min experimental recording epoch to measure spontaneous, convulsive 'seizure-like' swim behavior. Criteria for a positive hit with the threshold set at  $\geq -40\%$  mean velocity were based on previous standard deviations calculated from several DS larvae treated with plain embryo media [85].

All drug-treated larvae were run with controls from the same clutch on the same plate to ensure drug specificity. After the treatment paradigm or prolonged incubation periods, each larva was assessed for overall health, vehicle or drug-induced sedation/muscle relaxation, and drug-induced toxicity/deformities based on the criteria mentioned earlier [81,82,86]. The raw velocity values (mm/s) are first calculated by subtracting a larva's swim velocity after drug treatment from its baseline. This is multiplied by 100 to give the velocity (mm/s %change from baseline). A threshold for excluding negative values was not set in order to accurately capture the wide range of larval behavior at any given time during the assay and negative values could reflect immobility/lack of or limited larval movement during prolonged incubation periods inside the DanioVision observation chamber. For calculating percent increase or decrease in velocity, the formula, [Degree of increase or decrease/average velocity value of vehicle control]\*100 was used.

### 2.13. Microelectrode array (MEA) based electrophysiology

For performing MEA studies, the Axion Maestro system equipped with AxIS 2.5.2 software was used. Zebrafish brain recordings were performed based on studies previously done by Tomasello and Sive [87], Meyer M et al. [88,89], and Axion BioSystems (Axion Biosystems INC, Atlanta, GA, USA) with some modifications. The Axion Maestro was set at 28 °C for all zebrafish larvae studies. Low melting agarose (LMA) (1.5%) was dissolved in embryo media and kept melted on a heat block set at 95 °C. For the experiment, 6 dpf DS larvae were incubated with drugs/DMSO control for the required period. The final concentration of DMSO in all drug dilutions was less than 1%. 6-well CytoView MEA plates (Axion BioSystems- M348-Tmea-6B) with 64 poly (3,4-ethylenedioxythiophene) polystyrene sulfonate (PEDOT) electrodes/well were used for the zebrafish experiments. For every experiment, 5 wells in the plate were used and one larva was mounted/well. Out of the 5 wells, 3 wells had drug-treated larvae and 2 wells had DMSO-control larvae. A drop of agarose was added to the remaining well as technical control. For plating the larva, once agarose was cooled enough, a larva was quickly dropped and sucked up and then dropped gently onto the CytoView MEA well plate. This step was performed under a high magnification stereoscope and an eyelash tool was used to make sure that the larva was positioned in the correct orientation on the electrodes in each well. For detecting brain activity, we ensured that the larval head touched the electrode area in a way to best achieve array coverage. The larva was held flat with the eyelash tool until the agarose solidified. The CytoView plate was then placed in the recording chamber and real-time, spontaneous neural recordings were obtained for a 10min period. AxIS 2.5.2 software inbuilt within the MEA platform was utilized for data acquisition and analysis. The default settings for extracellular action potentials were used for neural spontaneous acquisition. The acquisition settings were as follows: Spike Detector was set at 5.5x STD; Burst Detector (inter-spike interval, ISI) was set at Maximum Inter Spike

Interval –100 ms and Minimum Number of Spikes-5 (Single Electrode Burst); Network Bursts were set at Maximum ISI-100 ms, Minimum Number of Spikes-3, Minimum Participating Electrodes- 3%; Mean Firing Rate Estimation was set at 10s; and Synchrony Parameters were set at 20 ms. After recording, the plate was placed back under the microscope to check if the larval orientation was unchanged and to note which numbered electrodes were in contact with the larval head region. Also, at this point, the immobilized larva was checked under a stereoscope for a normal heartbeat. Drug toxicity was assessed in a similar way as mentioned earlier. Data were analyzed using the Neural Metric Tool and batch processed. The batched data were processed through AxIS 2.5.2 with the denoted burst and network settings through the Statistics Compiler and the minimum threshold value for all parameters was set to be greater than 3% to be considered a reliable/true signal [87].

### 2.14. Statistical methods

Data were analyzed using GraphPad Prism software version 9.0 (San Diego, CA, USA). For comparisons between vehicle-treated control versus treatment groups, one-way ANOVA was utilized with Dunnett's multiple comparisons post-hoc test. For comparisons between all groups, a one-way ANOVA with Tukey's post-hoc test was performed. For all one-way ANOVA tests, the  $\alpha$  value was set at 0.05. For comparisons between two groups like vehicle-treated control versus drug treatment, the Student's unpaired *t*-test with Welch's correction was utilized.

## 3. Results

### 3.1. DMP elevates GSH and protects against 4AP-induced hyperexcitability and GSH depletion

Previous studies from our laboratory have shown that non-toxic concentrations of DMP (10–100  $\mu\text{M}$ ) increase intracellular GSH levels in microglial (BV2) cells and primary neuronal-glia cerebrocortical cultures after at least 4 h of incubation [21]. This increase in GSH inhibited the release of pro-inflammatory mediators from bacterial lipopolysaccharide (LPS)-stimulated BV2 cells [21]. Here, we determined whether DMP-mediated increase in intracellular GSH would attenuate 4AP-induced neuronal hyperexcitability in primary neuronal-glia cerebrocortical cultures. Mature (D14-D16) primary neuronal-glia cerebrocortical cultures were treated with either 30  $\mu\text{M}$  or 100  $\mu\text{M}$  DMP for 4 h followed by stimulation with 1 mM 4AP for 1 h. Neuronal excitability was measured by the high throughput MEA assay and extracellular action potential recordings were reported as number of spikes. By blocking the re-entry of potassium ( $\text{K}^+$ ) ions, 4AP prevents neuronal repolarization and propagates epileptiform activity [90]. 4AP (1 mM) was shown to be non-toxic up to 24 h and to elicit robust and sustained 'epileptiform-like' activity in primary neuronal-glia cerebrocortical cultures following incubation for 1 h in the MEA platform (Supplementary Figs. S1A and S1B). Cultures treated with 1 mM 4AP showed a significant increase (~372%) in the number of spikes compared to vehicle control. Cultures pre-incubated with either 30  $\mu\text{M}$  or 100  $\mu\text{M}$  DMP prior to 4AP stimulation showed a significant reduction (~40.5% for 30  $\mu\text{M}$  DMP + 4AP, and ~60.4% for 100  $\mu\text{M}$  DMP + 4AP groups respectively) in the number of spikes compared to the '4AP alone' group (Fig. 1A). DMP treatment alone did not alter basal levels of excitation compared to vehicle control. To verify whether the attenuation of 4AP-induced hyperexcitability in the DMP+4AP group was due to DMP-mediated increase in GSH, intracellular GSH and GSSG levels were measured in cultures subjected to the same treatment paradigm (4 h 30  $\mu\text{M}$  or 100  $\mu\text{M}$  DMP + 1 h 1 mM 4AP) in a separate experiment. Both 30  $\mu\text{M}$  and 100  $\mu\text{M}$  DMP significantly elevated intracellular GSH (~56.8% for 30  $\mu\text{M}$  DMP and ~48.1% for 100  $\mu\text{M}$  DMP groups respectively) (Fig. 1B) and total glutathione ( $\text{GSH} + 2^* (\text{GSSG})$ ) levels (Supplementary Fig. S1C) in these cultures compared to vehicle control.

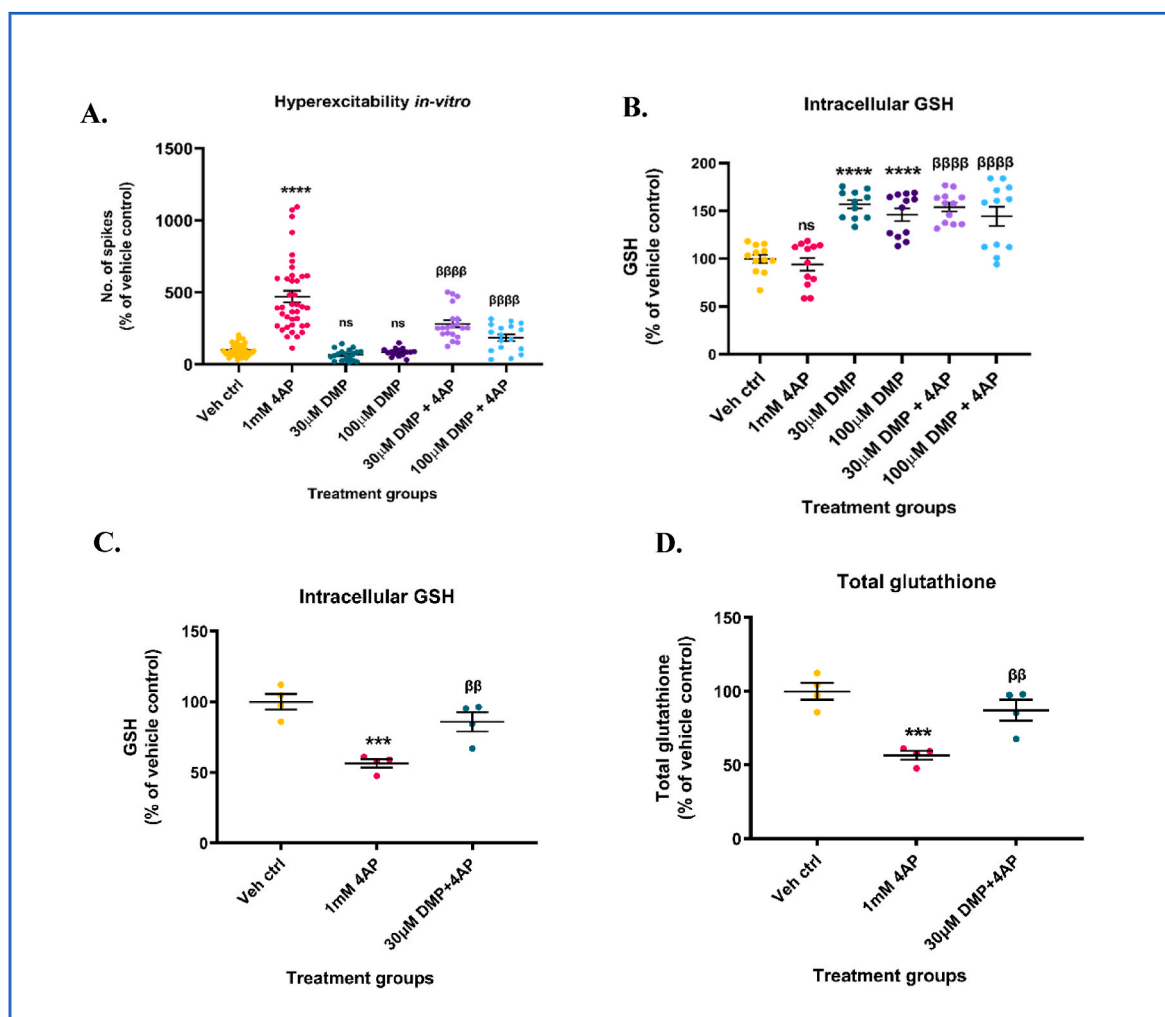


**Fig. 1. Dimercaprol (DMP) elevates intracellular GSH levels and protects against 4-aminopyridine (4AP)-induced neuronal hyperexcitability and GSH depletion.** Primary neuronal-glia cerebral cortical cultures were pretreated with either 30  $\mu$ M or 100  $\mu$ M dimercaprol for 4 h followed by 1 mM 4AP stimulation for 1 h following which extracellular action potentials (number of spikes), and reduced glutathione (GSH) levels were measured. (A) Number of spikes measured on MEA system (B) GSH levels measured by HPLC. Primary neuronal-glia cerebral cortical cultures were treated with 30  $\mu$ M DMP for 4 h followed by 1 mM 4AP treatment for 20 h. GSH and GSSG levels were measured by HPLC after the 24 h treatment paradigm. (C) GSH levels, and (D) Total glutathione (GSH+(2\*GSSG)) levels. Data are represented as mean  $\pm$  SEM (error bars). \*\*\*\* $p$  < 0.001, \*\*\*\* $p$  < 0.0001, ns: not significant versus vehicle control,  $\beta\beta$  $p$  < 0.01,  $\beta\beta\beta\beta$  $p$  < 0.0001 versus 1 mM 4AP by one-way ANOVA with Tukey's post-hoc test.  $n$  = 7–8/grp (A),  $n$  = 2–4/grp (B, C, and D).  $N$  = 3–4 experimental replicates. Mean  $\pm$  SD of raw data values of GSH normalized to total protein (nmol/mg protein) are stated in parentheses (GSH): a) Veh ctrl (13.6  $\pm$  7.4); b) 1 mM 4AP (11.9  $\pm$  4.1); c) 30  $\mu$ M DMP (20.9  $\pm$  10.7); d) 100  $\mu$ M DMP (19.7  $\pm$  9.6); e) 30  $\mu$ M DMP+4AP (20.9  $\pm$  10.2); and f) 100  $\mu$ M DMP+4AP (19.4  $\pm$  9.8) (1B); Mean  $\pm$  SD of raw data values of GSH and total glutathione normalized to total protein (nmol/mg protein) are stated in parentheses (GSH; total glutathione) for each treatment group: a) Veh ctrl (23.66  $\pm$  2.63; 23.76  $\pm$  2.68); 1 mM 4AP (13.35  $\pm$  1.43; 13.44  $\pm$  1.42); 30  $\mu$ M DMP+1 mM 4AP (20.29  $\pm$  3.22; 20.71  $\pm$  3.38) (1C and 1D).

Similarly, cultures pre-treated with either 30  $\mu$ M or 100  $\mu$ M DMP for 4 h prior to 4AP stimulation were able to significantly increase their GSH (~54% for 30  $\mu$ M DMP + 4AP, and ~44.2% for 100  $\mu$ M DMP + 4AP groups respectively) levels compared to the '4AP alone' group (Fig. 1B). 4AP treatment alone for 1 h did not alter GSH levels significantly compared to vehicle control. Treatment of primary neuronal-glia cerebral cortical cultures with 1 mM 4AP for 24 h significantly depleted GSH (~44%), and total glutathione (~56.6%) levels compared to vehicle control (Fig. 1C and D). Pre-treatment of cultures with 30  $\mu$ M DMP for 4 h prior to 4AP treatment for 20 h prevented the depletion of GSH (~52%) and total glutathione (~54%) levels compared to the '4AP alone' group (Fig. 1C and D). Taken together, these results indicate that the elevation of intracellular GSH levels using DMP prior to 4AP stimulation protected cultures from 4AP-induced hyperexcitability and hyperexcitability-induced GSH depletion.

Next, we tested the ability of another thiol-containing compound 3-mercapto-1-propanol (3MP) to inhibit 4AP-induced neuronal

hyperexcitability. In our previous study, the non-toxic concentration of 100  $\mu$ M 3MP has been shown to significantly elevate (~58%) intracellular GSH levels at 4 h compared to vehicle control [21]. Primary neuronal-glia cerebral cortical cultures were pre-treated with 100  $\mu$ M 3MP for 4 h followed by incubation with 1 mM 4AP for 1 h, and neuronal excitability was measured using the MEA assay. 4AP treatment significantly increased (~95.6%) the number of spikes compared to vehicle control. Cultures that received 100  $\mu$ M 3MP prior to 4AP stimulation showed a significant decrease (~48.8%) in the number of spikes compared to the '4AP alone group' (Supplementary Fig. S1D). 3MP treatment alone did not change basal levels of excitation (Supplementary Fig. S1D). This data suggests that the elevation of intracellular GSH levels by multiple thiol-containing compounds can attenuate neuronal hyperexcitability *in-vitro*.

### 3.2. 4AP-induced neuronal hyperexcitability activates mTORC1 in-vitro

To identify a redox-sensitive signaling pathway that may mechanistically link changes in cellular GSH levels with neuronal excitability, we examined the role of the mTOR pathway. Ample evidence from literature has shown that the mTORC1 pathway is aberrantly activated in genetic [40], and acquired experimental models [91,92] and resected brain tissue [93,94] from human epilepsy patients. Also, oxidative stress has been shown to hyperactivate mTORC1 in several other disease pathologies [95,96] and neurotoxicant-mediated neurodegeneration [97]. Since 4AP treatment depleted GSH, we asked if treatment with 4AP could hyperactivate mTORC1 and whether pre-treatment with DMP prior to 4AP treatment could attenuate this. Primary neuronal-glial cerebrocortical cultures were treated with 30  $\mu$ M DMP for 4 h followed by treatment with 1 mM 4AP for an additional 4 h. Treatment time for 4AP was determined from pilot studies (data not shown). To ascertain that the mTORC1 pathway in our cultures was functional and detectable, 20 nM rapamycin, an allosteric inhibitor of mTOR kinase activity was used as a positive control [43,44]. Moreover, rapamycin and its analogs (e.g., everolimus) are used to treat pediatric patients with medically refractory epilepsies [98–100] and would serve as a clinically relevant positive control. The cytotoxicity of rapamycin at 24 h was determined by an LDH release assay (Supplementary Fig. S2A). Antimycin A (10  $\mu$ M), an inhibitor of mitochondrial complex III (CIII) which is known to increase steady-state superoxide ( $O_2^-$ ) levels was used as a positive control. At the concentrations tested in our study, rapamycin did not exert detectable cell injury at 24 h following incubation, whereas antimycin A significantly increased (~81.5%) LDH release in media compared to vehicle control (Supplementary Fig. S2A). mTORC1 kinase activity was assessed by measuring the phosphorylation of one of its downstream targets, the S6 ribosomal protein. Protein levels of phospho-S6 and total S6 were measured by immunoblotting. 4AP treatment alone activated mTORC1 by ~55.3% compared to vehicle control. Pre-treatment with DMP significantly attenuated (~28.0%) mTORC1 hyperactivation compared to the '4AP alone' group (Fig. 2A and B). DMP alone did not alter mTORC1 activity significantly. Rapamycin treatment significantly decreased (~88.5%) mTORC1 activity compared to vehicle control. To further investigate the involvement of the mTORC1 pathway in regulating neuronal excitability, primary

neuronal-glial cerebrocortical cultures were treated with 20 nM rapamycin for 8 h followed by stimulation with 1 mM 4AP for 1 h after which neuronal excitability was measured by the MEA assay. Stimulation with 1 mM 4AP alone significantly increased (~393.1%) the number of spikes compared to the vehicle control group. Interestingly, incubation with 20 nM rapamycin prior to 4AP stimulation significantly attenuated (~36.4%) 4AP-induced neuronal hyperexcitability compared to the '4AP alone' group (Supplementary Fig. S2B). It is important to note that rapamycin treatment by itself did not alter neuronal excitability. Taken together, these results suggest that 4AP-induced neuronal hyperexcitability activates mTORC1 and pre-treatment with DMP that elevates GSH or rapamycin, an mTORC1 inhibitor attenuates this in primary neuronal-glial cerebrocortical cultures.

### 3.3. Intracellular GSH depletion hyperactivates mTORC1 in-vitro

The mTORC1 pathway consists of several redox-sensitive proteins that integrate a variety of cellular cues including oxidative stress, changes in metabolite concentrations, bioenergetic status, and subsequently orchestrate a multitude of cellular responses [31]. To better understand how alterations in intracellular GSH levels impact mTORC1 activity, we asked if GSH depletion using BSO would adversely affect mTORC1 activity *in-vitro*. BSO is a potent, specific, and irreversible inhibitor of GCL, the rate-limiting enzyme in GSH biosynthesis. Specifically, GCL catalyzes the phosphorylation of BSO in the presence of magnesium ( $Mg^{2+}$ ) and adenosine triphosphate (ATP), and the resulting product, buthionine sulfoximine phosphate, irreversibly binds to and inhibits GCL [101,102]. Non-toxic concentrations of BSO (10, 30, 100 and, 300  $\mu$ M) were selected based on data from an LDH release assay (Supplementary Fig. S3A). Antimycin A (10  $\mu$ M) was used as a positive control. BSO concentrations tested were non-toxic at 24 h. Antimycin A significantly increased (~51.2%) LDH release in media compared to vehicle control (Supplementary Fig. S3A). Primary neuronal-glial cerebrocortical cultures were treated with increasing doses of BSO for 24 h and intracellular GSH, GSSG levels were measured by HPLC. At 24 h, cultures treated with increasing doses of BSO showed a significant decrease in reduced glutathione (~52.7%, 60.4%, 70.6%, and 73.2% for 10, 30, 100, and 300  $\mu$ M BSO respectively) and total glutathione (~50.9%, 55.9%, 66.8%, and 72% for 10, 30, 100, and 300  $\mu$ M BSO

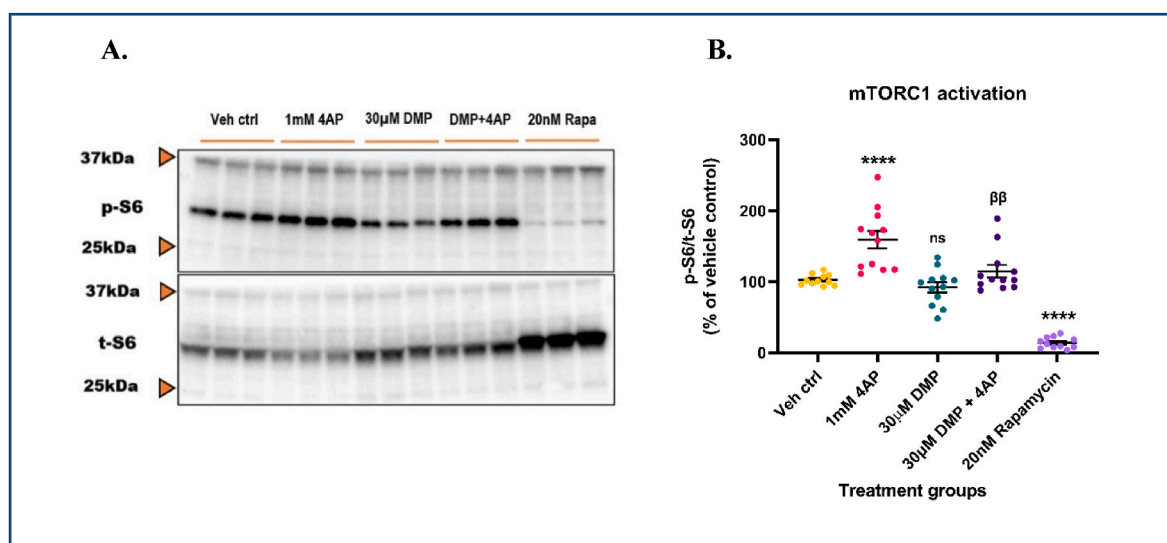


**Fig. 2.** 4AP-induced hyperexcitability aberrantly activates mTORC1. Primary neuronal-glial cerebrocortical cultures were pretreated with 30  $\mu$ M dimercaprol for 4 h and then stimulated with 1 mM 4AP for an additional 4 h. mTORC1 activity represented by phospho-S6 (p-S6)/total S6 (t-S6) was assessed by immunoblotting. 20 nM rapamycin was used as procedural/positive control. (A) Representative blot, and (B) Blot quantification. Data are represented as mean  $\pm$  SEM (error bars). \*\*\*\* $p < 0.0001$ , ns: not significant versus vehicle control,  $\beta\beta p < 0.01$  versus 1 mM 4AP by one-way ANOVA with Tukey's post-hoc test.  $n = 3$ /grp.  $N = 4$  experimental replicates.

respectively) levels compared to vehicle control (Fig. 3A and B). GSSG levels were also significantly depleted in the cultures after BSO treatment (Supplementary Fig. S3B). BSO treatment for 24 h did not alter the GSH redox status, as assessed by the GSH/GSSG ratio (Supplementary

Fig. S3C).

Next, we assessed how this GSH depletion affected the phosphorylation of the S6 ribosomal protein. This experiment was conducted in serum-free and serum-containing MEM media to rule out the influence

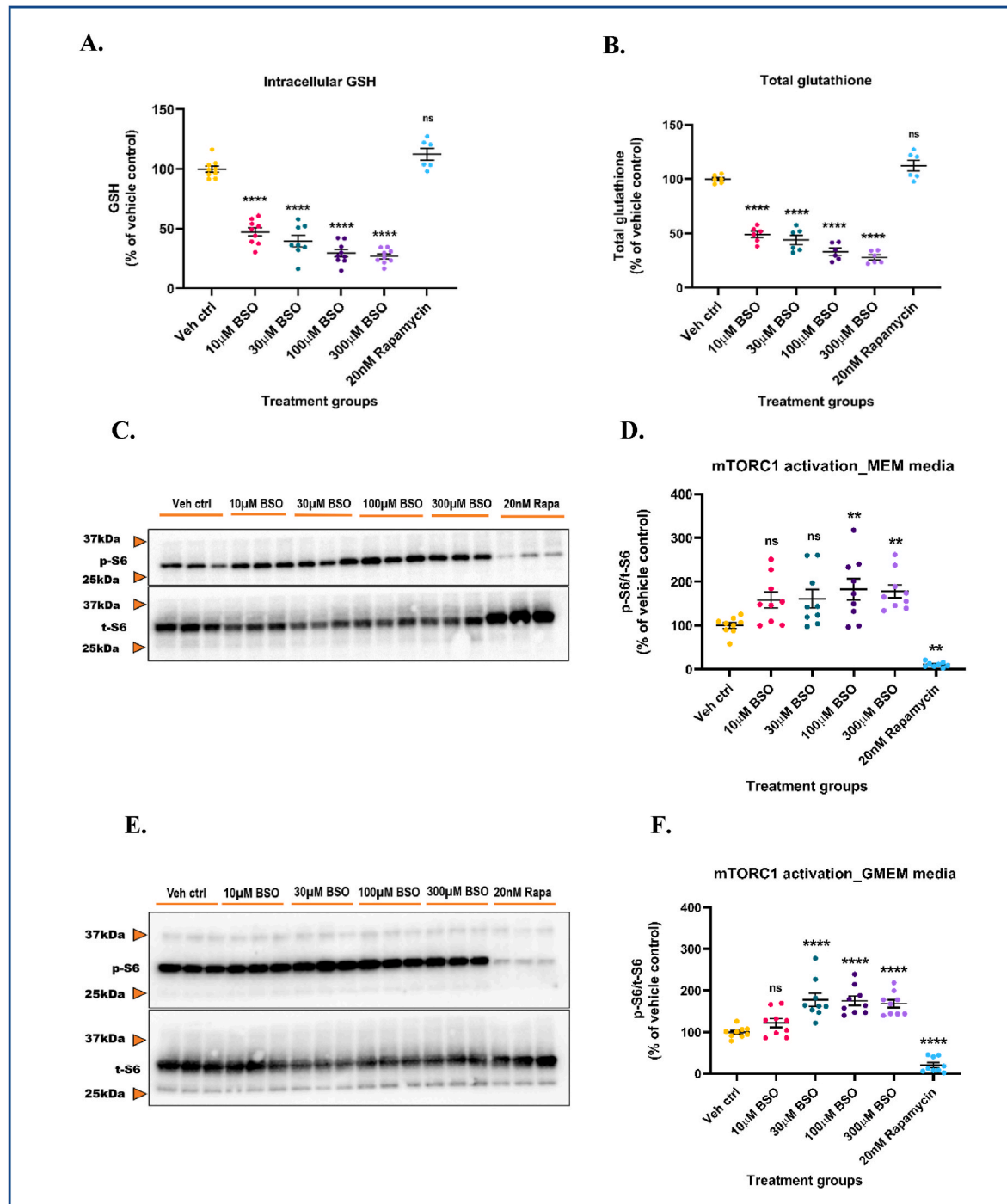


**Fig. 3. Intracellular GSH depletion aberrantly activates mTORC1 in both serum-free and serum-containing media.** Primary neuronal-glia cerebrocortical cultures were treated with increasing concentrations of L-thionine-(S,R)-sulfoximine (BSO) in MEM media and GSH, GSSG levels were measured by HPLC. 20 nM rapamycin was used as an additional negative control for this experiment. (A) GSH levels and (B) Total glutathione levels. Cultures were treated with increasing BSO concentrations for 24 h in MEM (serum-free) (C and D) or GMEM (serum-containing) (E and F) media and mTORC1 activity represented by p-S6/t-S6 was assessed by immunoblotting. (C) Representative mTORC1 immunoblot (MEM media), and (D) Blot quantification. (E) Representative mTORC1 immunoblot (GMEM media), and (F) Blot quantification. 20 nM rapamycin was used as procedural/positive control for the immunoblotting experiments. Data are represented as mean ± SEM (error bars). \*\**p* < 0.01, \*\*\*\**p* < 0.0001, ns: not significant *versus* vehicle control by one-way ANOVA with Dunnett's post-hoc test (A, B, D and F). *n* = 3/grp. *N* = 3 experimental replicates. Mean ± SD of raw data values of GSH and total glutathione normalized to total protein (nmol/mg protein) are stated in parentheses (GSH; total glutathione) for each treatment group: a) Veh ctrl (6.3 ± 4.9; 9.5 ± 2.0); b) 10 µM BSO (3.0 ± 2.3; 4.6 ± 0.6); c) 30 µM BSO (3.0 ± 1.9; 4 ± 0.3); d) 100 µM BSO (2.0 ± 1.5; 3.0 ± 0.3); e) 300 µM BSO (1.7 ± 1.3; 2.6 ± 0.2); and f) 20 nM Rapamycin (10.4 ± 1.1; 10.5 ± 1.1) (3A and 3B).

of serum components as a possible explanation for mTORC1 activation. Cultures were treated with increasing doses of BSO for 24 h in serum-free MEM media and phospho/total S6 ribosomal protein levels were assessed by immunoblotting. As GSH levels were progressively depleted, phosphorylation of S6 significantly increased in a reciprocal manner (~57.9%, 60.9%, 82.5%, and 78.0% for 10, 30, 100, and 300  $\mu$ M BSO respectively) compared to vehicle control. 20 nM rapamycin used as a positive control significantly decreased S6 phosphorylation (~89.4%) compared to vehicle control (Fig. 3C and D). To ensure that this activation of mTORC1 was primarily due to GSH depletion by BSO, we determined mTORC1 activation in response to GSH depletion in serum-containing MEM media (GMEM). Cultures were treated with BSO for 24 h and phospho/total S6 levels were assessed by immunoblotting. Even in serum-containing media, GSH depletion significantly increased phosphorylation of S6 (~22.4%, 77.8%, 75.4%, and 68.6% for 10, 30, 100, and 300  $\mu$ M BSO respectively) compared to vehicle control (Fig. 3E and F). One explanation for the absence of dose-response in S6 phosphorylation could be the possible interference from serum components that could have influenced the uptake of BSO. Additionally, the strong activation of mTORC1 at a lower dose (30  $\mu$ M) in GMEM media could be attributed to the presence of serum albumin protein and growth factors that are known to activate mTORC1 [103,104]. However, when basal levels of mTORC1 activation in serum-free and serum-containing media were compared, no significant changes were observed (data not shown). Rapamycin (20 nM) significantly inhibited (~90.6%) mTORC1 compared to vehicle control even under serum-containing media conditions. To avoid possible interactions between added compounds and serum components, subsequent experiments were conducted in serum-free MEM media. Finally, to ascertain that rapamycin-induced changes in S6 phosphorylation were not mediated by alterations in intracellular GSH levels, GSH levels in the 20 nM rapamycin treated cultures were measured by HPLC. No significant changes in reduced and total glutathione levels were observed compared to vehicle control (Fig. 3A and B). These data suggest that the depletion of intracellular GSH levels can trigger the aberrant activation of mTORC1 in the presence/absence of serum components suggesting a potential redox-based mechanism.

### 3.4. Reciprocal modulation of mTORC1 activity by GCL-driven GSH levels

Redox-sensitive proteins in the mTORC1 pathway have several key cysteine residues that may be susceptible to alterations in the cellular redox tone [56,57,105]. One of the key functions of GSH is to act as a reductant and protect vulnerable protein thiols from irreversible oxidative/nitrosative modifications [16,106]. Depletion of GSH may cause the cellular redox environment to become more oxidized thereby leading to alterations in protein structure and function [107–109]. Depletion of intracellular GSH by GCL inhibition resulted in the activation of mTORC1 in primary neuronal-glia cerebrocortical cultures as assessed by phospho-S6/total S6 levels. We next determined if DMP pre-treatment prior to BSO treatment would attenuate mTORC1 hyperactivation. Briefly, primary neuronal-glia cerebrocortical cultures were pre-treated with 30  $\mu$ M DMP for 4 h to allow for the increase in GSH by GCL activation. After 4 h, cultures were treated with 100  $\mu$ M BSO for 20 h to inhibit GCL and halt further production of GSH. 20 nM rapamycin was used as a positive control. Protein levels of phospho-S6, and total S6 were assessed by immuno-blotting. 100  $\mu$ M BSO treatment significantly increased (~37.4%) mTORC1 activity compared to vehicle control. Cultures pre-treated with DMP prior to BSO treatment showed a significant decrease (~32.3%) in mTORC1 activity compared to the 'BSO alone' group. 'DMP alone' insignificantly altered mTORC1 activity compared to vehicle control. 20 nM rapamycin significantly decreased (~91.5%) mTORC1 compared to vehicle control (Fig. 4A and B). Taken together, these data strongly suggest that the modulation of intracellular GSH levels *via* GCL can influence the activity of mTORC1 *in-vitro*. In addition, these data indicate that DMP pre-treatment prior to BSO treatment can attenuate mTORC1 hyperactivation in primary neuronal-glia cerebrocortical cultures.

### 3.5. Intracellular GSH depletion oxidatively modifies tuberous sclerosis proteins TSC1, TSC2, and TBC1D7

Tuberous sclerosis proteins TSC1, TSC2, and TBC1D7 are critical, upstream negative regulators of mTORC1 activity [54,110] and are cysteine-rich [57]. Earlier studies have demonstrated that an oxidized

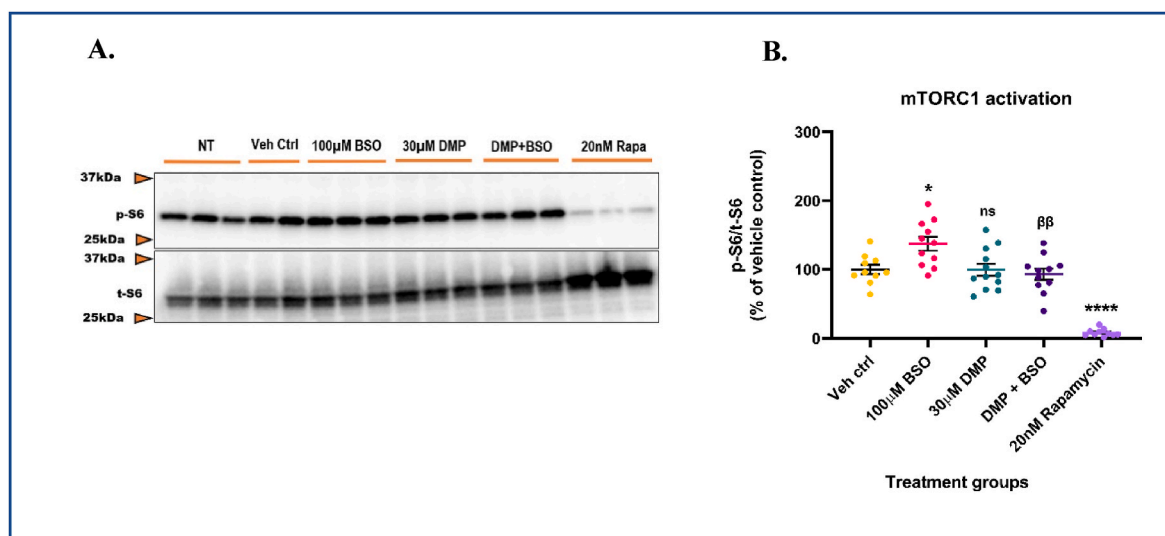


**Fig. 4. GSH depletion hyperactivates mTORC1 and its repletion protects against aberrant mTORC1 activation.** Primary neuronal-glia cerebrocortical cultures were pre-treated with 30  $\mu$ M dimercaprol for 4 h followed by 100  $\mu$ M BSO treatment for 20 h in MEM media. 20 nM rapamycin was used as procedural/positive control. mTORC1 activity represented by p-S6/t-S6 was assessed by immunoblotting. No treatment control (NT) represents primary neuronal-glia cerebrocortical cultures treated with plain serum-free MEM media. This control was run to assess basal mTORC1 activity in the cultures and it was not significantly different ( $P = 0.4767$ ) compared to the vehicle control group. (A) Representative mTORC1 immunoblot, and (B) Blot quantification. Data are represented as mean  $\pm$  SEM (error bars). \* $p < 0.05$ , \*\*\*\* $p < 0.0001$ , ns: not significant versus vehicle control;  $\beta\beta p < 0.01$  versus 100  $\mu$ M BSO by one-way ANOVA with Tukey's post-hoc test.  $n = 2-3$ /grp.  $N = 4$  experimental replicates.

cellular redox environment can lead to mTORC1 hyperactivation even under amino-acid depleted conditions. These studies also showed that the presence of the TSC protein complex was essential for oxidants to exert their effects (i.e., mTORC1 hyperactivation) [57]. Since GSH depletion increased mTORC1 activity in our cultures, we asked if redox-based modifications to TSC proteins played a role in exerting this effect. To address this question, we determined the degree of oxidation of TSC proteins under GSH depleted conditions by the redox western-blotting technique. This technique was initially optimized by conducting a pilot study with the oxidant phenylarsine oxide (PAO) and reductant dithiothreitol (DTT). PAO is a trivalent arsenical that specifically complexes with vicinal sulfhydryl groups in proteins and is known to induce oxidative stress [111,112]. DTT is a dithiol containing small

molecule that reduces disulfides in a two-step thiol-disulfide exchange reaction [113]. Primary neuronal-glia cerebrocortical cultures were treated with either 1  $\mu$ M PAO or 1 mM DTT for 30min and probed for TSC1 and  $\beta$ -tubulin.  $\beta$ -tubulin was chosen as the loading control based on a previously published study [114] which showed that the treatment of neuroblastoma cells with high concentrations of BSO (5 mM, or 12.5 mM) for 24 h affected the actin cytoskeletal network but not  $\beta$ -tubulin. Although  $\beta$ -tubulin has been shown by some studies to interact with GSH and form GSH-tubulin mixed disulfides, this interaction has been shown to occur at high (i) temperatures (30  $^{\circ}$ C) [115]; (ii) concentrations of GSH (~5 mM) [116]; and (iii) levels of steady-state ROS [116]. The concentration and duration of treatment for PAO and DTT were selected from previous studies in literature where they were shown to be

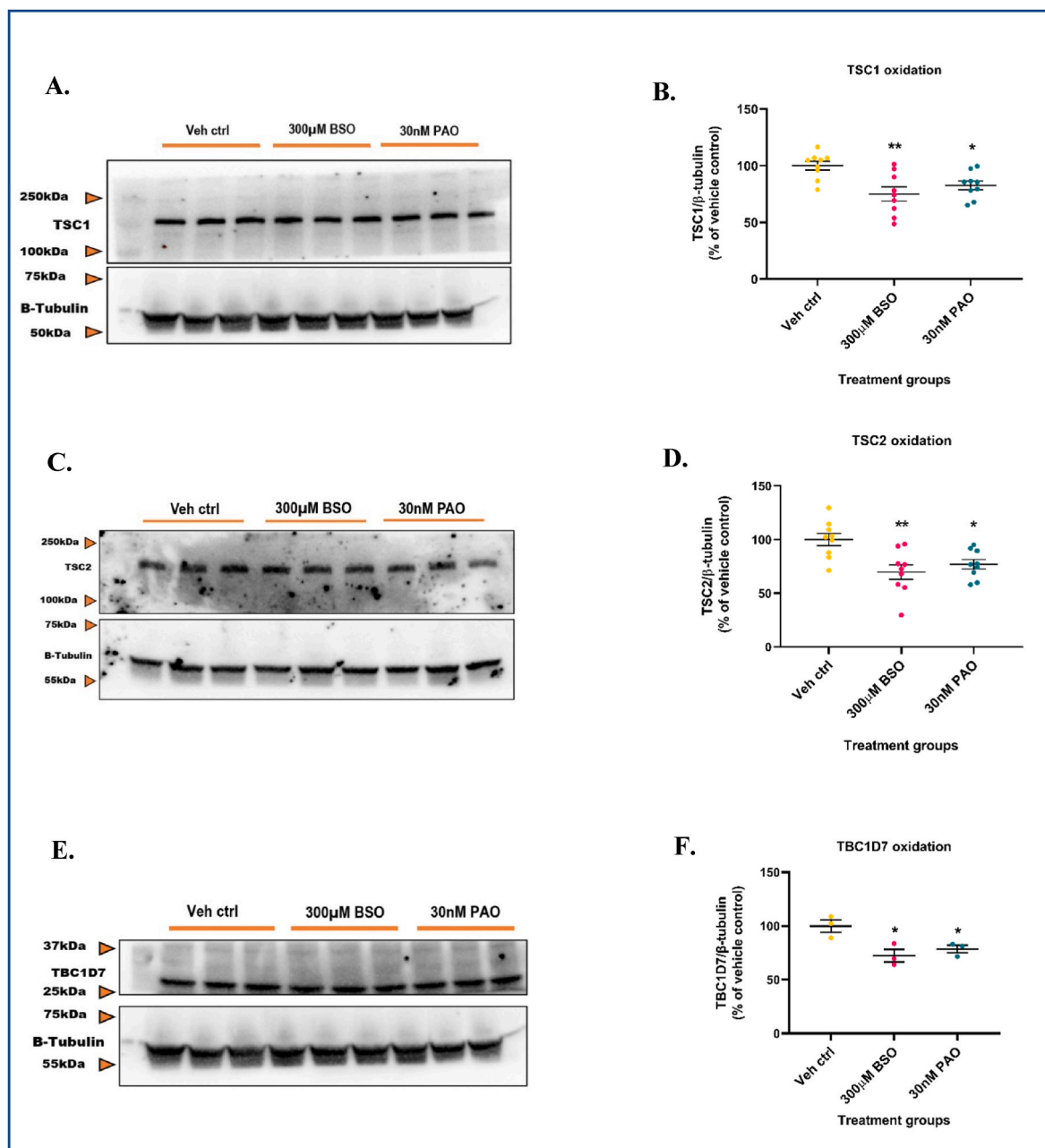


**Fig. 5.** GSH depletion oxidizes TSC1, TSC2, and TBC1D7 in the mTORC1 pathway. Primary neuronal-glia cerebrocortical cultures were treated with 300  $\mu$ M BSO for 24 h and the total proteins TSC1, TSC2, and TBC1D7 normalized to loading control  $\beta$ -tubulin were probed for by redox-western blotting. 30 nM PAO was used as positive control. (A) Representative blot, and (B) Blot quantification for TSC1. (C) Representative blot, and (D) Blot quantification for TSC2. (E) Representative blot, and (F) Blot quantification for TBC1D7. Data are represented as mean  $\pm$  SEM (error bars). \* $p$  < 0.05, \*\* $p$  < 0.01 versus vehicle control by one-way ANOVA with Dunnett's post-hoc test.  $n$  = 3/grp.  $N$  = 3 experimental replicates.

non-toxic [57,117,118]. Only the oxidant treated bands showed significantly less density (~64.5%) compared to vehicle control (Supplementary Figs. S4A and S4B). The banding pattern from DTT treatment was not significantly different (~18.2%) compared to vehicle control. Also, no significant changes in band mobility or intensity were observed for  $\beta$ -tubulin. This indicated that even after treatment with a potent oxidant like PAO or a reductant like DTT,  $\beta$ -tubulin did not undergo significant redox-mediated changes such as the formation of mixed disulfides with GSH or tubulin polymerization. Such changes generally affect antibody avidity (alteration in band intensity) and/or cause a shift in protein molecular weight (mobility shift). The lack of changes in  $\beta$ -tubulin's band intensity and band mobility compared to vehicle control indicated that  $\beta$ -tubulin was resistant to redox-mediated changes at the concentrations of PAO and DTT used and hence could serve as a reliable loading control. Therefore, this pilot study helped select the appropriate loading, and positive controls, understand/visualize the banding pattern of oxidized proteins, and quantify the resulting band intensities to determine percent oxidation.

Next, we conducted redox blotting experiments with BSO and PAO. 300  $\mu$ M BSO was selected since it depleted intracellular GSH levels to >70% and was non-toxic to primary neuronal-glia cerebral cortical cultures at 24 h. An LDH release assay for increasing concentrations (3, 10, 30, and 100 nM) of PAO was performed to select a non-toxic concentration that could be used as a positive control for a 24 h treatment (Supplementary Fig. S4C). The 3, 10, and 30 nM PAO concentrations were non-toxic whereas 100 nM PAO significantly increased (~38.9%) LDH release in media at 24 h compared to vehicle control. The positive control, 10  $\mu$ M antimycin A significantly increased (~52%) LDH release in media compared to vehicle control.

Primary neuronal-glia cerebral cortical cultures were treated with 300  $\mu$ M BSO or 30 nM PAO for 24 h followed by measurement of total protein (normalized to  $\beta$ -tubulin) and estimation of percent oxidation of target proteins (TSC1, TSC2, and TBC1D7). Quantification of band intensities of TSC1, TSC2, and TBC1D7 in the BSO and PAO treated groups and comparison with vehicle control revealed that the vehicle control always had higher values (~85%–120%) compared to the BSO (~40%–90%), and PAO (~60%–95%) treated groups normalized to  $\beta$ -tubulin. This trend in data was consistent across all experimental replicates. Interestingly, the results indicated that ~20–30% each of TSC1 (~20.1%), TSC2 (~30.3%), and TBC1D7 (~27.6%) (Fig. 5A–F) were oxidatively modified compared to vehicle control after treatment with BSO for 24 h. About 17.3% of TSC1, 23.1% of TSC2, and 21.4% of TBC1D7 were oxidatively modified compared to vehicle control when treated with PAO (Fig. 5A–F). These data suggest that the maintenance of intracellular GSH levels is critical for the regulated functioning of proteins in the mTORC1 pathway. Depletion of GSH levels to greater than 50% can oxidize key regulatory proteins in this pathway thereby leading to a hyperactive mTORC1 in primary neuronal-glia cerebral cortical cultures. A schematic of the proposed mechanism by which GCL-mediated modulation of intracellular GSH levels by either BSO or DMP could influence mTORC1 activity is represented in Supplementary Fig. S5A.

### 3.6. DMP elevates GSH and attenuates acute 'seizure-like' swim behavior in wildtype (WT) zebrafish larvae

To test DMP's ability to elevate GSH levels and attenuate hyperexcitability *in-vivo*, we chose a zebrafish model of hyperexcitability. Larval zebrafish are exceptionally amenable to genetic manipulation and along with a fully mapped out glial/neuronal transcriptome [119,120], whole brain connectome [121,122], and GSH redox dynamics [123], they have become a model of choice for understanding seizure mechanisms, tracking whole brain seizure activity, and for high-throughput screening of potential antiseizure drugs. The use of a 4AP zebrafish model would have been more appropriate for the transition from *in-vitro* to *in-vivo* studies. However, we chose to use the PTZ acute zebrafish seizure model

since it has been shown to exhibit consistent, and robust, 'ictal-like' events unlike the 4AP zebrafish model which exhibits only non-seizure hyperexcitable states even after prolonged exposure to high concentrations of 4AP (4 mM) [124]. The goal for our *in-vivo* studies was to assess whether DMP-mediated increases in GSH would significantly attenuate true, robust 'ictal-like' events in an acute seizure model. To model acute seizures in humans, the larval pentylentetrazol (PTZ) model of acute 'seizure-like' behavior was developed, well-characterized at the behavioral, molecular, and electrographic levels, and validated using existing anticonvulsant drugs [125,126]. Also, data from rodent PTZ models showed a reduction in seizures when treated with NAC, a GSH precursor [127]. We first used wildtype (WT) zebrafish larvae. 5-7 dpf WT larvae were treated with increasing concentrations (1, 10, 30, and 100  $\mu$ M) of DMP for 4 h, and GSH, GSSG levels were measured by HPLC. The concentrations and treatment duration were chosen based on results obtained from *in-vitro* studies and the absence of observable adverse effects in larvae. Only 100  $\mu$ M DMP significantly increased both reduced (~68.03%) (Fig. 6A) and total glutathione (~63.7%) (Supplementary Fig. S6B) levels compared to vehicle control. GSSG levels were not significantly altered in DMP treated larvae (Supplementary Fig. S6A).

Next, we determined if this increase in GSH levels would attenuate PTZ-induced acute 'seizure-like' swim behavior in WT larvae. Larvae were pretreated with 100  $\mu$ M DMP for 4 h followed by stimulation with 10 mM PTZ for 40min. Treatment duration and non-toxic concentration of PTZ (GABA-A receptor antagonist) were chosen from previous studies that have extensively characterized PTZ treated WT larvae at the behavioral, molecular, and electrographic levels [125,126]. PTZ treated larvae exhibit changes in swim behavior, and tonic-clonic seizures [125, 126]. These changes in locomotion/swim behavior were assessed by the high-throughput Noldus DanioVision system running the EthoVisionXT software. This system tracks larval movement, calculates distance moved and velocity, and correlates these indices to 'seizure-like' swim behavior [81,128]. One plausible reason for negative values observed in the vehicle control and 'DMP only' groups could be attributed to very limited larval movement during prolonged incubation periods inside the DanioVision observation chamber. Larvae treated with 10 mM PTZ showed a significant increase (~905.9%) in acute 'seizure-like' swim behavior compared to vehicle control. Such large measures of larval swim velocity post-PTZ treatment have been observed in a previous study which used the ZebraBox infrared tracking system [129]. Surprisingly, larvae pre-treated with DMP and then stimulated with PTZ showed a significant decrease (~39.5%) in acute 'seizure-like' swim behavior compared to the 'PTZ alone' group (Fig. 6B). DMP treatment by itself did not significantly alter the locomotion behavior of larvae compared to vehicle control (Fig. 6B). These data suggest that GSH elevation using DMP protected WT zebrafish larvae from PTZ-induced acute 'seizure-like' swim behavior.

### 3.7. DMP increases GSH and inhibits spontaneous 'seizure-like' swim behavior in Dravet Syndrome (*scn1Lab*) mutants

Since DMP was successful in elevating GSH and attenuating PTZ-induced acute 'seizure-like' swim behavior, we asked if DMP would exert its effects in mutant Dravet Syndrome (DS, *scn1Lab*) zebrafish larvae. The reasons for utilizing the DS larvae for our initial *in-vivo* studies were three-fold: (i) The *scn1Lab* larval zebrafish mutants identified from a chemical mutagenesis screen have been used to study and develop/repurpose drugs for DS [81,130]; (ii) the DS larvae exhibit spontaneous 'seizure-like' behavior that could be utilized as a first-stage behavior screen for DMP's dose-response studies; and (iii) DS larvae exhibit robust electrographic seizures, a critical endpoint that could be used to assess DMP's ability to attenuate spontaneous epileptiform discharges.

DS, also known as Severe Myoclonic Epilepsy of Infancy (SMEI) is a catastrophic, drug-resistant, pediatric epilepsy with a high rate of mortality, prolonged and frequent early-life seizures, severe intellectual

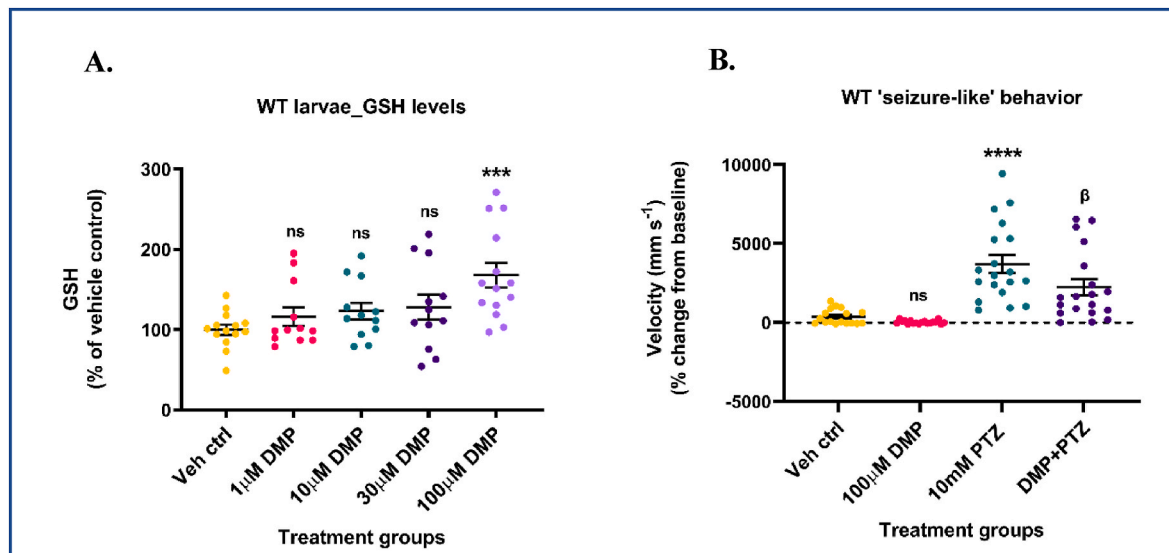


**Fig. 6.** Dimercaprol increases GSH and attenuates acute 'seizure-like' swim behavior in wildtype larvae. 5-7 dpf wildtype (WT) zebrafish larvae were treated with 1, 10, 30 or 100  $\mu$ M dimercaprol for 4 h. GSH levels were measured by HPLC. (A) Larval GSH levels. WT larvae were pre-treated with 100  $\mu$ M DMP for 4 h and stimulated with 10 mM PTZ for 40 min. Larval locomotion/swim behavior was measured by the Noldus DanioVision system running the EthoVisionXT software. (B) Change in larval swim velocity correlated to 'seizure-like' behavior. Data are represented as mean  $\pm$  SEM (error bars). \*\*\* $p$  < 0.001, \*\*\*\* $p$  < 0.0001, ns: not significant versus vehicle control;  $\beta$  $p$  < 0.05 versus 10 mM PTZ by one-way ANOVA with Dunnett's post-hoc test (A) and Tukey's post-hoc test (B).  $n$  = 50–70 larvae pooled/grp (HPLC assay) and  $n$  = 10 larvae/grp (Noldus assay).  $N$  = 4–5 experimental replicates. Mean  $\pm$  SD of raw data values of GSH normalized to total protein (nmol/mg protein) are stated in parentheses (GSH) for each treatment group: a) Veh ctrl (14.9  $\pm$  7.7); b) 1  $\mu$ M DMP (14.9  $\pm$  5.9); c) 10  $\mu$ M DMP (16.2  $\pm$  6.9); d) 30  $\mu$ M DMP (15.5  $\pm$  4.7); and e) 100  $\mu$ M DMP (21.7  $\pm$  5.4) (6A).

disability, and psychomotor dysfunction [131,132]. In 80–90% of the cases, DS is caused by *de novo* mutations in the *SCN1A* gene that encodes a voltage-gated sodium channel (Na<sub>v</sub> 1.1) subunit [131]. The *scn1Lab* mutants accurately recapitulate phenotypic characteristics of human DS

patients wherein they exhibit early-life, convulsive and drug-resistant seizure behavior, spontaneous electrographic seizures, premature death, metabolic deficits, and movement disorders [80,81]. 5-7 dpf *scn1Lab* mutants were treated with increasing concentrations (10, 30,

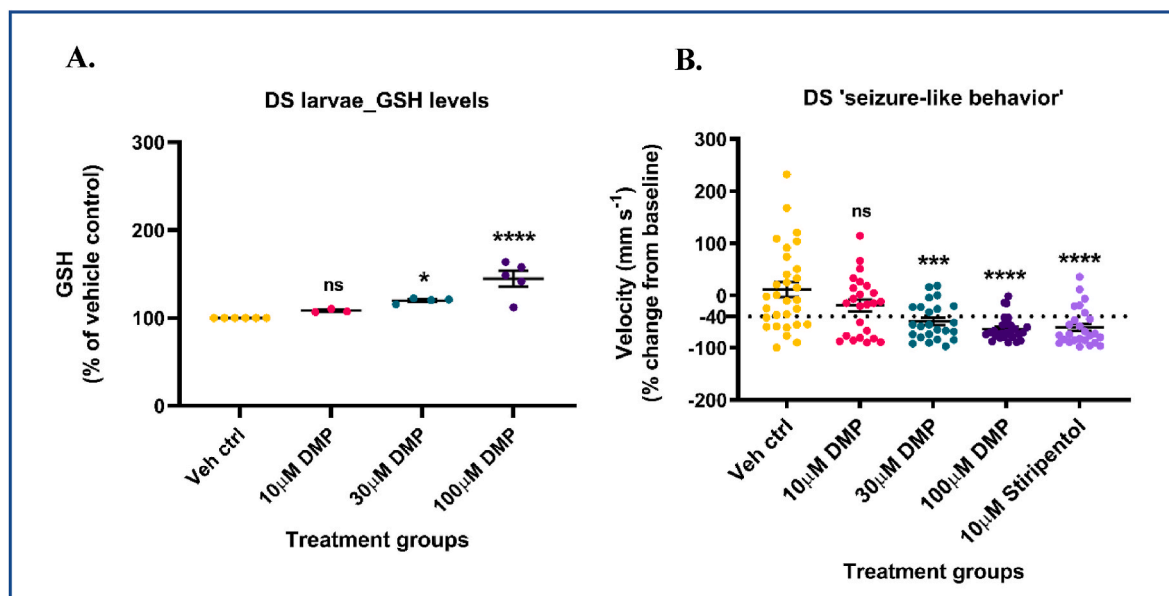


**Fig. 7.** Dimercaprol increases GSH levels and inhibits spontaneous 'seizure-like' swim behavior in DS (*scn1Lab*) mutants. 5-7 dpf *scn1Lab* mutants were treated with 10, 30 or 100  $\mu$ M dimercaprol for 4 h. GSH levels were measured by HPLC. (A) DS mutants' GSH levels. DS mutants were treated with increasing concentrations of DMP for 4 h and swim behavior was assessed by the Noldus DanioVision system running the EthoVisionXT software. 10  $\mu$ M stiripentol was used as a positive control. (B) Change in larval swim velocity correlated to 'seizure-like' behavior. The dotted black line at  $\sim$  -40% represents the cut-off point below which velocity values corresponding to larval swim behavior are considered significantly reduced. Data are represented as mean  $\pm$  SEM (error bars). \* $p$  < 0.05, \*\*\* $p$  < 0.001, \*\*\*\* $p$  < 0.0001, ns: not significant versus vehicle control by one-way ANOVA with Dunnett's post-hoc test (A and B).  $n$  = 50–70 larvae pooled/grp (HPLC assay) and  $n$  = 10 larvae/grp (Noldus assay).  $N$  = 4–5 experimental replicates. Mean  $\pm$  SD of raw data values of GSH normalized to total protein (nmol/mg protein) are stated in parentheses (GSH) for each treatment group: a) Veh ctrl (14.2  $\pm$  2.7); b) 10  $\mu$ M DMP (15.2  $\pm$  4.4); c) 30  $\mu$ M DMP (16.3  $\pm$  2.4); and d) 100  $\mu$ M DMP (19.8  $\pm$  2.0) (7A).

and 100  $\mu\text{M}$ ) of DMP for 4 h and GSH, GSSG levels were measured by HPLC. DS mutants treated with 30  $\mu\text{M}$  DMP showed a significant increase in GSH (~19.9%) (Fig. 7A) and total glutathione (~19.4%) (Supplementary Fig. S7B) levels compared to vehicle control. Additionally, DS larvae treated with 100  $\mu\text{M}$  DMP showed the highest increase in GSH (~44.8%) (Fig. 7A) and total glutathione (~44.2%) (Supplementary Fig. S7B) levels compared to vehicle control. No significant changes were observed in GSSG levels compared to vehicle control (Supplementary Fig. S7A). Also, the high degree of variance observed in GSSG values could be due to two plausible reasons: (i) GSSG is present in femtomolar ranges in a zebrafish larva [133] and given the very limited yield of DS mutants from a single clutch, pooling sufficient larvae for reliable detection of GSSG using HPLC becomes exceedingly difficult; (ii) defects in pigment aggregation that have been reported in DS mutants [81] could have interfered with the detection of GSSG in samples.

To determine if DMP treatment would inhibit spontaneous 'seizure-like' swim behavior, DS mutants were treated with increasing concentrations (10, 30 and, 100  $\mu\text{M}$ ) of DMP for 4 h and larval swim behavior was measured by using the Noldus DanioVision system running the EthoVisionXT software. DS mutants have been reported to exhibit spontaneous, unprovoked, whole-body convulsions and drug compounds were considered successful in this assay if they reduced mutant behavior to (i) very little swim activity; or (ii) increased, but non-convulsive swim activity [81,126]. Non-toxic dose of 10  $\mu\text{M}$  stiripentol, an allosteric modulator of the GABA-A receptor and a clinically approved drug to treat DS patients was used as a positive control [134, 135]. Swim velocity values below (or greater than) -40% will be considered a significant inhibition of DS larval movement. This threshold was chosen based on an earlier study [136] that determined a baseline standard deviation of ~17.5% acquired from several DS mutants treated with plain embryo media. This study considered drugs to be a positive hit only if they reduced swim velocity values to greater than -40% (2X standard deviation). Some negative values observed in the vehicle control group could be attributed to limited larval movement during prolonged incubation periods inside the DanioVision observation chamber. To clearly differentiate between the effects of the drug (DMP) versus vehicle (DMSO) on DS larval 'seizure-like' behavior, a secondary validation assay that measures electrographic activity from larval brain was performed as a next step. 100  $\mu\text{M}$  DMP (dose that most significantly increased GSH levels) treated larvae showed the greatest reduction (~644.9%) in 'swim velocity' compared to vehicle control (Fig. 7B). Larvae treated with 30  $\mu\text{M}$  DMP (second most potent dose) showed a significant reduction (~524.3%) in 'swim velocity' compared to vehicle control. Such changes in DS larval swim velocity in response to various antiseizure medications has been observed in a previous study that utilized the Noldus DanioVision for tracking locomotion [81]. Both 30  $\mu\text{M}$  and 100  $\mu\text{M}$  DMP significantly decreased spontaneous and convulsive 'seizure-like' swim behavior in DS mutants to levels comparable to Stage 0 or Stage 1 (reduced mean swim velocity) in the locomotion assay. Stiripentol significantly (~621.1%) reduced the swim velocity of the mutants compared to vehicle control (Fig. 7B). Taken together, these results suggest that even the acute elevation of GSH levels in DS mutants can attenuate spontaneous, and convulsive 'seizure-like' swim behavior.

### 3.8. DMP elevates GSH and attenuates spontaneous electrographic seizures in DS (*scn1Lab*) mutants

To determine if GSH elevation in DS larvae suppressed spontaneous electrographic seizures, we measured EEG-like signals/extracellular action potentials from the larval nervous system using the non-invasive MEA platform. EEG-like signals correspond to electrical discharges or potentials which are recorded as relative changes in voltage in the extracellular space around neurons [87]. These signals can be recorded in multiple configurations ranging from single electrode recordings to multielectrode arrays [137]. The use of MEA platforms for recording

EEG-like signals from the zebrafish larval nervous system has been validated by previous studies [87–89]. Using a custom-made MEA platform, Meyer M et al. [88,89] showed that chemoconvulsant-induced epileptic seizures can be measured non-invasively from multiple larval brain regions with spatial and temporal resolution. The addition of 15 mM potassium chloride (KCl) or 15 mM PTZ to the bath of intact larvae significantly increased seizure parameters such as extracellular action potentials (no. of spikes), burst rate, and synchrony compared to the untreated control group.<sup>88,89</sup> This study highlights the sensitivity/capability of the MEA platform to differentiate between epileptiform discharges arising from a non-synaptic (KCl) versus trans-synaptic (PTZ) seizure model. Tomasello DL and Sive H<sup>87</sup> used a commercially available MEA platform (Axion Biosystems) to measure EEG-like signals and other seizure parameters including electrographic burst events, and network activity in 7 dpf larvae treated with 500  $\mu\text{M}$  valproic acid, an anticonvulsant drug. Treatment with valproic acid significantly decreased the number of spikes, mean spike rate, average number, frequency, and percentage of electrographic burst events without significant changes to network activity. In our study, DS mutants were treated with either 100  $\mu\text{M}$  DMP or vehicle control for 4 h followed by the recording of spontaneous 'seizure-like' activity for 1 h with 10min recording epochs on the MEA platform. To accurately evaluate seizure activity, Axion's MEA system measures parameters such as number of spikes, mean spike rate, number of electrographic burst events, electrographic burst frequency, and synchrony index. 100  $\mu\text{M}$  DMP treated DS mutants showed a significant reduction in number of spikes (~63.4%) (Fig. 8A), mean spike rate (~83.1%) (Fig. 8B), the number of electrographic burst events (~61.2%) (Fig. 8C), and electrographic burst frequency (~62.4%) (Fig. 8D) compared to vehicle control. DMP treatment did not alter the synchrony index compared to vehicle control (Fig. 8E) most likely because we conducted our recordings only for 1 h, whereas the measurement of synchrony of large neuronal networks is often measured over much longer periods of time and the fluctuations are averaged to obtain the final data [138–140]. Two positive controls were used in this study for rigor and validation of recordings obtained from the MEA system. Stiripentol (10  $\mu\text{M}$  for 4 h), a clinically-approved second-line/add-on antiseizure medication for DS patients, significantly decreased swim velocity of DS mutants in the Noldus behavior assay and inhibited the number of spikes (~79.2%) (Fig. 8A), mean spike rate (~88.7%) (Fig. 8B), and the number of electrographic burst events (~83%) (Fig. 8C), but not electrographic burst frequency (Fig. 8D) or synchrony index (Fig. 8E) compared to vehicle control. PK11195, a translocator protein (TSPO) ligand and gluconeogenesis activator via phosphoenolpyruvate carboxykinase 1 (*pck1*), was recently shown to reverse metabolic deficits and suppress spontaneous electrographic seizures in *scn1Lab* mutants and was chosen as an independent positive control [86]. Treatment of DS mutants with a non-toxic dose of PK11195 (10  $\mu\text{M}$ ) for 4 h significantly decreased the number of spikes (~78.5%) (Fig. 8A) compared to vehicle treatment. These results confirm previous studies with PK11195 [86] or stiripentol [81] showing significantly attenuated spontaneous electrographic seizures in DS mutants assessed by invasive single-electrode-based extracellular field recordings (Fig. 8A).

Taken together, these data suggest that GSH elevation using DMP can attenuate both convulsive 'seizure-like' swim behavior and spontaneous electrographic seizures in a genetic model of pediatric, pharmacoresistant epilepsy. In addition, these data highlight the use of the behavior assay as a 'first-pass' screening tool for assessing the anticonvulsant property of new compounds and underscore the importance of secondary methods (invasive or non-invasive electrographic recording) of validation [125,136].

## 4. Discussion

Maintenance of intracellular GSH levels is critical in brain cells, especially neurons that are susceptible to seizure-induced oxidative

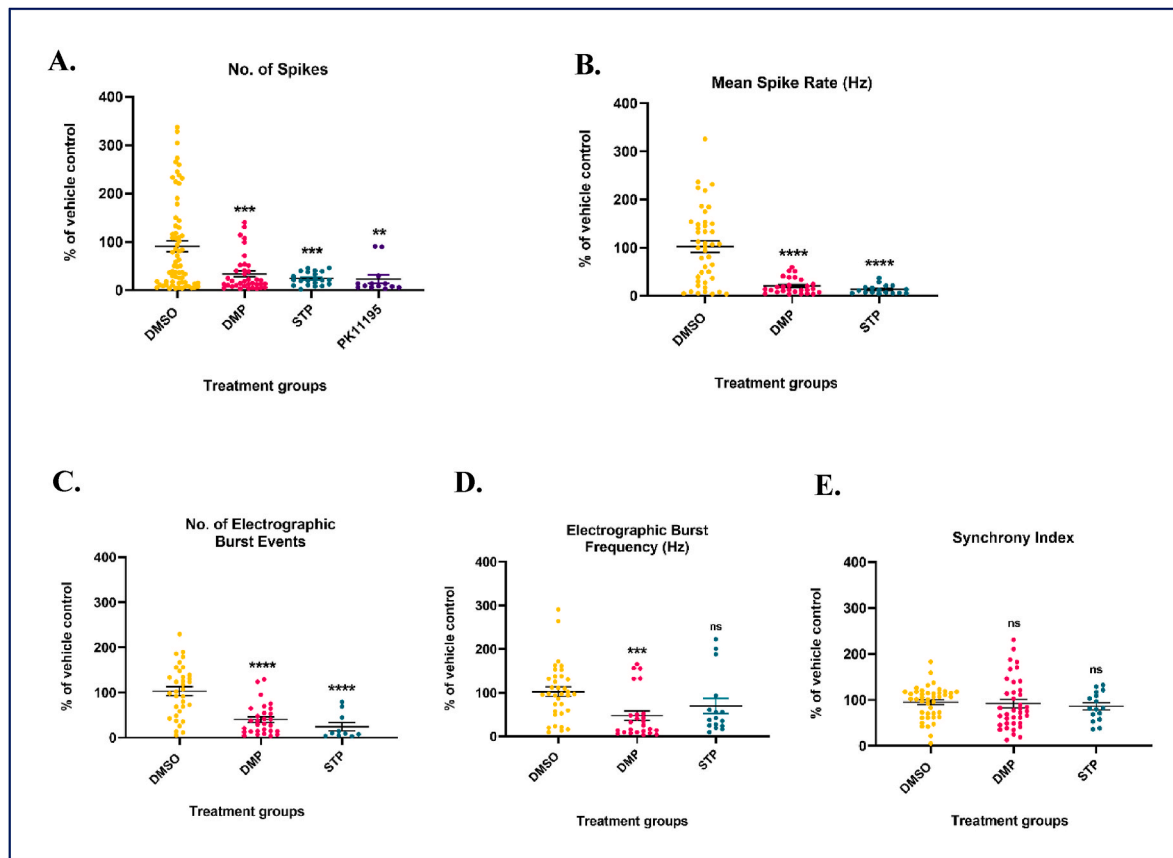


**Fig. 8.** Dimercaprol treatment significantly decreases a series of ‘seizure-like’ parameters in DS (*scn1Lab*) mutants. DS mutants were treated with 100  $\mu$ M dimercaprol for 4 h. Dimethyl sulfoxide (DMSO,  $\sim$ 1%) was used as vehicle control. 10  $\mu$ M stiripentol (STP), and 10  $\mu$ M PK11195 were used as positive controls. (A) No. of spikes, (B) Mean spike rate, (C) Number of electrographic burst events, (D) Electrographic burst frequency, and (E) Synchrony index were assessed by the Axion MEA system. The minimum threshold value for all parameters was set to be greater than 3% to be considered a reliable/true signal. Data are represented as mean  $\pm$  SEM (error bars). \*\* $p < 0.01$ , \*\*\* $p < 0.001$ , \*\*\*\* $p < 0.0001$ , ns: not significant *versus* vehicle control by one-way ANOVA with Dunnett’s post-hoc test.  $n = 3$ –5 larvae/grp.  $N = 10$  experimental replicates.

stress, and bioenergetic fluctuations, and have limited antioxidant capacity (e.g., reduced catalase activity). Since GSH can scavenge a variety of cellular RS (particularly  $H_2O_2$ ), and act as a substrate for antioxidant enzymes like GPx, GST, Grx, neurons require it mainly to scavenge  $H_2O_2$ , remove lipid hydroperoxides, prevent ferroptosis, and protect protein sulfhydryl’s from irreversible oxidation [17,141–143]. Extensive evidence from literature and studies from our laboratory have shown that the increase in intracellular GSH levels predominantly by Nrf2-dependent mechanisms can decrease oxidative stress and the release of pro-inflammatory mediators, increase seizure threshold, and rescue certain cognitive deficits [20,21,24,25,144]. Additionally, the KD a high fat/low carbohydrate diet used to treat patients with refractory epilepsy is known to exert its anticonvulsant effects in part *via* the activation of Nrf2 which improves mitochondrial and tissue redox state [145]. However, how the modulation of GSH redox status controls neuronal hyperexcitability remains unclear. Several key findings emerged from this study. *First*, a thiol-containing compound, DMP which has been shown to post-translationally activate the GSH biosynthetic enzyme GCL, elevated intracellular GSH levels in primary neuronal-glia cerebral cortical cultures and attenuated neuronal hyperexcitability. *Secondly*, DMP attenuated hyperexcitability-induced mTORC1 activation. *Third*, modulation of intracellular GSH levels either by pharmacological inhibition of GCL by BSO or activation by DMP significantly influenced mTORC1 activity *in-vitro*. *Fourth*, the depletion of intracellular GSH levels oxidatively modified tuberous sclerosis proteins, TSC1, TSC2, and TBC1D7 in the mTORC1 pathway. *Finally*, DMP-mediated GSH elevation inhibited convulsant-induced and spontaneous

‘seizure-like’ swim behavior in WT and DS zebrafish larvae respectively. DMP also attenuated spontaneous electrographic seizures in DS mutants with chronic epilepsy. To the best of our knowledge, this study is the first of its kind to demonstrate that thiol-containing compounds such as DMP which are capable of elevating GSH levels, can inhibit neuronal hyperexcitability *in-vitro* and *in-vivo*. Together, these studies also suggest a novel redox-based mechanism to control hyperexcitability/seizures arising from acquired or genetic origins.

To model neuronal hyperexcitability *in-vitro*, we used 4AP, a voltage-gated potassium channel blocker that blocks the re-entry of potassium ( $K^+$ ) ions and prevents neuronal repolarization thereby extending action-potential firing [90]. Several reasons make 4AP a good candidate for inducing hyperexcitability reminiscent of ‘epileptiform activity’ in primary neuronal-glia cerebral cortical cultures: (i) unlike glutamate receptor agonists, 4AP does not cause excitotoxic neuronal cell death in primary cultures [146], and this was verified in our culture system where 1 mM 4AP did not release LDH up to 24 h; (ii) the *in-vitro* 4AP model of acute ‘seizure-like’ activity has been robustly used to elucidate the efficacy of many antiseizure drugs [147]; (iii) 4AP is extensively used to induce acute generalized tonic-clonic convulsions with systemic/parenteral administration [148–152] or focal, hypersynchronous, high-amplitude epileptiform discharges with focal application [149, 153–155] in rodents; and (iv) 4AP evoked ‘seizure-like’ activity *in-vitro* is clinically relevant owing to several 4AP overdose and accidental poisoning cases resulting in seizures in humans [156,157]. In this study, the treatment of primary neuronal-glia cerebral cortical cultures with 1 mM 4AP for 1 h evoked robust hyperexcitability which was significantly

inhibited by DMP (30  $\mu$ M or 100  $\mu$ M) pre-treatment for 4 h. Cultures that received DMP prior to 4AP stimulation had significantly higher levels of intracellular GSH compared to the '4AP alone' group. Also, prolonged treatment (20 h) with 1 mM 4AP significantly decreased intracellular GSH levels in cerebrocortical cultures which was prevented by pre-treatment with DMP (30  $\mu$ M). Potassium channel antagonists including 4AP are known to induce oxidative stress in different model systems such as rodent brains [158,159] and cancer cells [160]. In the brain, 4AP mediated increase in calcium influx [161], mitochondrial membrane potential [158,159], mitochondrial respiration [80], and glutamatergic neurotransmission [162,163] are key processes that induce oxidative stress which in turn can further perpetuate epileptiform activity. This is supported by studies where naturally-occurring antioxidant compounds have been shown to decrease 4AP-induced oxidative burden, offer neuroprotection, and in some cases, attenuate seizure activity [159]. In the present study, it is highly likely that DMP mediated increase in GSH protected cerebrocortical cultures from hyperexcitability and GSH depletion by attenuating 4AP-induced oxidative stress. This could also explain why DMP treatment prior to 4AP stimulation rescued cultures from hyperexcitability but DMP by itself did not alter basal excitation since these cultures would not have been burdened by 4AP-induced oxidative stress. These findings are supported by previous studies which have shown that seizures can cause oxidative stress, and chronic GSH depletion in the brains of animal models [9,10,13,164] and human patients [15]. Treatment with compounds/therapies that increase GSH levels such as SFN [20,22,165], NAC [22,166], DMF [25,167], and KD [168–170] have been shown to significantly decrease oxidative stress and increase seizure threshold in rodent models and human epilepsy patients.

A dysregulated mTORC1 pathway is another deleterious process that occurs concomitantly with oxidative stress and chronic GSH depletion and is widely implicated in the pathogenesis of epilepsy. mTORC1 senses stimuli such as oxidative stress, growth factors, amino acids, and metabolic/bioenergetic status of the cell [31,49,171–173]. Acute and chronic activation of mTORC1 has been observed in several acquired [33,35,91,174], genetic epilepsy models [39,94,175,176] and resected brain tissue from epilepsy patients [177–179]. In the present study, treatment of primary neuronal-glia cerebrocortical cultures with 1 mM 4AP for 4 h significantly increased mTORC1 activation which was attenuated by DMP (30  $\mu$ M) pre-treatment for 4 h. Since 4AP-induced hyperexcitability has been reported to induce oxidative stress, this likely contributed to the hyperactivation of mTORC1. In cultures that received DMP prior to 4AP treatment, elevated GSH levels could have protected against oxidative-stress mediated hyperactivation of mTORC1. This is in line with a recent study where the convulsant pilocarpine-induced *status epilepticus* (SE) resulted in hyperactivation of mTORC1 in rat hippocampus and piriform cortex [34]. Treatment with a small molecule reactive oxygen species (ROS) scavenger post SE significantly attenuated mTORC1 hyperactivation thereby suggesting the involvement of seizure-induced ROS in mTORC1 dysregulation [34].

Next, we used two approaches that directly tested the involvement of GCL in modulating the mTORC1 pathway. The first approach involved inhibition of GCL using BSO which resulted in a steep decline in GSH levels accompanied by activation of the mTORC1 pathway in both serum-free and serum-containing media. Conversely, DMP treatment, which was previously shown to increase GCL holoenzyme formation, elevated GSH levels and prevented BSO mediated mTORC1 hyperactivation suggesting a mechanistic link between alterations in intracellular GSH levels and mTORC1 activity. These findings are consistent with a previous study where kainic acid treated rats showed a significant increase in mTORC1 activation in the hippocampus and neocortex [180]. It is important to note that kainate-induced SE has been shown by an earlier study to cause chronic GSH depletion in the rat hippocampus [9]. Intriguingly, this activation was significantly decreased after initiation of the KD post SE in kainate-treated rats [180]. The KD has been shown to work in part in rodent models by increasing the activity of

GSH-related enzymes such as GCL, GPx [181], and by increasing mitochondrial GSH levels [145,168,169]. A recent study in pediatric epilepsy patients highlighted the increase in brain GSH levels after treatment with the KD [170]. In another study that supports our findings, T lymphocytes (T cells) obtained from systemic lupus erythematosus (SLE) patients had severely decreased GSH levels and a hyperactive mTOR. However, T cells from SLE patients treated with NAC had significantly higher levels of GSH and decreased mTOR activity [182].

We have shown that BSO-mediated depletion of intracellular GSH to >50%, oxidatively modified TSC proteins in the mTORC1 pathway in primary neuronal-glia cerebrocortical cultures. The TSC proteins contain several cysteine residues in structural domains of association between TSC1, TBC1D7, and TSC2 and in the functional GAP domain of TSC2 [110,183]. Redox-mediated alterations of such cysteinyl residues could result in structural destabilization of the TSC protein complex thereby leading to the impairment in TSC2's Rheb-GTPase activity which could cause persistent activation of mTORC1. Overt GSH depletion has been shown by several studies to make the cellular redox tone more oxidative which could adversely impact protein thiols involved in redox-sensitive signal transduction [184–186]. BSO treatment can deplete intracellular GSH in a dose and time-dependent manner [187]. A previous study showed that a 24 h treatment with 1 mM BSO caused a moderate increase in steady-state ROS levels (particularly  $H_2O_2$ ) compared to the control group which was mitigated by pre-treatment with a reductant like DTT in a B cell lymphoma cell line (PW) [187]. This could offer a likely explanation for how GSH depletion led to the oxidation of TSC proteins in our study. PAO used a positive control in our study oxidatively modified TSC proteins plausibly by oxidizing vicinal thiol groups found as CXXC motifs in these proteins. These findings are congruent with studies that have shown quite paradoxically that oxidants can hyperactivate mTORC1 under nutrient-deprived conditions and reductants can attenuate mTORC1 under nutrient-rich conditions [56,57]. These studies also highlighted the role of the TSC protein complex in the redox-mediated regulation of mTORC1 by demonstrating the failure of an oxidant and reductant to alter mTORC1 activity and the subsequent phosphorylation of downstream ribosomal S6 kinase (S6K) in TSC1 and TSC2 knockout fibroblasts [57].

Larval zebrafish treated with seizurogenic agents elicit robust and quantifiable 'seizure-like' behavior, electrographic seizures, and molecular/biochemical alterations comparable to those observed in rodent models [125,126]. The ease of genetic manipulation along with the availability of different strains has facilitated the generation/development of larvae that develop epilepsy and exhibit spontaneous seizures [81,86]. This implies that the larval zebrafish brain is susceptible to seizure development and both genetic and chemical-induced larval seizure models have been well-characterized and utilized for screening antiseizure drug compounds [128,188,189]. In our study, DMP elevated GSH levels in both WT and DS larvae thus suggesting that DMP may have worked by acting on the GSH biosynthetic enzyme GCL. This is supported by studies which have shown that zebrafish larvae carry single copies of the genes *gclc* and *gclm* that are required to make the protein subunits of GCL [190]. Elevation of GSH levels in WT larvae attenuated PTZ-induced acute 'seizure-like' swim behavior. This is consistent with studies where pre-treatment with antioxidant phytochemicals like curcumin and gastrodin has been shown to attenuate PTZ-induced acute 'seizure-like' swim behavior. Interestingly, these two compounds work in part by increasing GSH levels and decreasing oxidative stress [191,192]. This is also congruent with findings from rodent models that demonstrate the ability of the GSH precursor, NAC to decrease PTZ-induced oxidative stress and clonic generalized seizures [127,193]. Furthermore, the KD that is known to work in part by elevating GSH levels has been shown to significantly enhance resistance to PTZ-induced seizures in rodent models [194,195].

DS is a rare, epileptic encephalopathy that is highly pharmacoresistant and associated with a high rate of sudden unexpected death in epilepsy (SUDEP) [131,196,197]. Currently available treatment options

inadequately control seizures and associated comorbidities, and hence there is an unmet need for the identification/development of effective antiseizure drugs [198]. In the present study, both 30  $\mu$ M and 100  $\mu$ M DMP increased GSH levels and attenuated spontaneous, convulsive 'seizure-like' swim behavior in a dose-dependent manner in DS mutants. One plausible explanation for the dose-response observed in DS mutants but not in wildtype larvae could be attributed to defects in pigmentation [81] that could have altered drug uptake owing to pigment aggregation. Another plausible explanation could be attributed to the DS mutants having spontaneous seizures starting at around 3 dpf [81] that could have potentially altered blood-brain barrier (BBB) permeability to drugs. Moreover, 100  $\mu$ M DMP's effect on DS larval swim behavior was comparable to the effect of stiripentol that was used as a positive control. These results are consistent with studies that have shown that the KD which works in part by increasing GSH levels by a Nrf2-dependent mechanism, can significantly rescue metabolic deficits [80] and attenuate convulsive 'seizure-like' swim behavior [81] in DS mutants. DMP treatment significantly attenuated several parameters associated with spontaneous electrographic seizures in the DS mutants. This is reminiscent of the KD-mediated suppression of spontaneous epileptiform discharges in DS mutants assessed by the invasive, single-electrode-based extracellular field recording [81,199]. The KD has been shown to effectively decrease seizure frequency and improve quality of life in patients with DS [200–202]. Although the exact mechanisms underlying KD-mediated seizure control are unclear, pivotal animal [145,168] and clinical studies [170] have shown that ketone bodies as a fuel source increased brain GSH levels which could confer antioxidant, and neuroprotective effects.

Stiripentol, and PK11195, the two positive controls used in the MEA study have different mechanisms of action compared to DMP and were successful in suppressing spontaneous electrographic seizures in DS mutants. This could indicate the involvement of varied underlying pathogenic mechanisms that could be the cause and consequence of 'seizure-like' behavior and associated comorbidities in DS mutants. This is supported by insights from clinical practice where combinatorial therapies are the norm for treating pharmacoresistant DS patients. This includes the use of (i) antiseizure medications (ASMs) that increase the GABAergic tone like valproate, stiripentol, or decrease glutamatergic neurotransmission like topiramate [203], and (ii) dietary therapies like the KD that induce metabolic changes, enhance bioenergetic reserves, and improve the antioxidant capacity of the brain [204]. Future studies that explore the exact mechanism by which DMP-mediated GSH elevation attenuates 'seizure-like' swim behavior and electrographic seizures in DS mutants are warranted.

**Limitation:** This study has several limitations. 1) Previous studies have shown that DMP can increase intracellular GSH levels in all cell types which possess the biosynthetic machinery for GSH [21] including primary neuronal-glia cerebrocortical cultures, microglia (BV2 cells), and dopaminergic neurons (N27 cells) [21]. Primary neuronal-glia cerebrocortical cultures comprise of large excitatory neuronal and glial populations but contain only a small number of GABAergic neurons/interneurons. Understanding the role of cell-type specific changes in GSH redox status and their influence on hyperexcitability, while important was beyond the scope of this study. 2) Treatment of DS mutants for 6 h with 300 nM rapamycin, an allosteric mTORC1 inhibitor, did not inhibit 'seizure-like' behavior and electrographic seizures (data not shown). However, this does not eliminate the possibility that treatment of DS mutants with a different dose/duration of rapamycin or its analog, everolimus, would attenuate spontaneous 'seizure-like' behavior and electrographic seizures. Although the exact mechanism of how DMP attenuated 'seizure-like' behavior/electrographic seizures in DS larvae is yet to be delineated, the possible involvement of the mTOR pathway warrants future studies. 3) We utilized the Axion MEA system for measuring spontaneous electrographic seizures in DS mutants. However, it is important to acknowledge that the MEA platform comes with certain inherent limitations such as movement artifacts, and the

limited ability of planar two-dimensional electrodes to capture on-going network activity from a three-dimensional model system such as the intact zebrafish larval brain. Single-electrode-based local field potential (LFP) recordings are the 'gold standard' and the ultimate confirmatory method for assessing electrographic seizures in zebrafish larvae [81, 199].

## 5. Conclusion

We have demonstrated that GSH elevation using the small molecule thiol-containing drug DMP can attenuate neuronal hyperexcitability by improving cellular redox tone and inhibiting hyperactive mTORC1 *in-vitro*. Modulation of intracellular GSH levels by a novel mechanism offers a way to control mTORC1 activation *in-vitro*. Moreover, the identification of TSC proteins in the mTOR pathway to be susceptible to GSH depletion makes them potential targets worthy of evaluation for anti-epileptogenic/antiseizure effects. Finally, the ability of DMP to attenuate seizures in the DS zebrafish model suggests the utility of this class of compounds for the treatment of catastrophic epilepsies such as DS.

## Author contributions

M.P., and A.S.H. conceived the idea of the project. A.S.H., R.B., L.P., R.E.F., C.Q.H., P.B.M., and T.F. conducted all the experiments and analyzed the data. J.R.R provided resources, helped with the experimental set-up, and data analysis for redox western blots. A.S.H., and M. P., wrote the paper.

## CRedit authorship contribution statement

Conceptualization: **Manisha Patel, and Ashwini Sri Hari**. Methodology: **Ashwini Sri Hari, Rajeswari Banerji, James R. Roede, and Manisha Patel**. Investigation: **Ashwini Sri Hari, Rajeswari Banerji, Li-Ping Liang, Ruth E. Fulton, Christopher Quoc Huynh, Timothy Fabisiak, and Pallavi Bhuyan McElroy**. Validation: **Li-Ping Liang, Ruth E. Fulton**. Resources: **Timothy Fabisiak, Christopher Quoc Huynh, James R. Roede, Manisha Patel**. Writing – Original draft, review, and editing: **Ashwini Sri Hari, and Manisha Patel**. Funding acquisition: **Manisha Patel**.

## Ethics approval and consent to participate

Our studies were carried out in strict accordance with the recommendations in the Guide for the Care and Use of Laboratory Animals of the National Institutes of Health (NIH). All procedures were approved by the Institutional Animal Care and Use Committee (IACUC) of the University of Colorado Denver (UCD), which is fully accredited by the Association for Assessment and Accreditation of Laboratory Animal Care (AAALAC).

## Funding

This work was supported by funding from the National Institutes of Health (NIH) [grant numbers R01NS086423, R37NS039587, R01HD102071, NIH/NCATS Colorado CTSA UL1 TR002535 (TM Pilot awards)].

## Declaration of competing interest

The authors declare that they have no known competing financial interests or personal relationships that could have appeared to influence the work reported in this paper.

## Data availability

Data will be made available on request.

## Acknowledgments

The authors thank Dr. Scott Baraban (University of California (UCSF)) for kindly providing the Dravet Syndrome (DS) heterozygous (*scn1Lab<sup>+/-</sup>*) parent (male and female) lines. The authors would also like to thank Eric Warren for his efforts on standardizing extracellular action potential recordings from primary neuronal-glia cerebral cortical cultures on the Axion MEA system.

## Appendix A. Supplementary data

Supplementary data to this article can be found online at <https://doi.org/10.1016/j.redox.2023.102895>.

## References

- [1] I.E. Scheffer, S. Berkovic, G. Capovilla, et al., ILAE classification of the epilepsies: position paper of the ILAE commission for classification and terminology, *Epilepsia* 58 (4) (2017) 512–521.
- [2] M.J. England, C.T. Liverman, A.M. Schultz, L.M. Strawbridge, Epilepsy across the spectrum: promoting health and understanding. A summary of the Institute of Medicine report, *Epilepsy Behav.* 25 (2) (2012) 266–276.
- [3] L. Dalic, M.J. Cook, Managing drug-resistant epilepsy: challenges and solutions, *Neuropsychiatr Dis Treat* 12 (2016) 2605–2616.
- [4] P. Kwan, A. Arzimanoglou, A.T. Berg, et al., Definition of drug resistant epilepsy: consensus proposal by the ad hoc Task Force of the ILAE Commission on Therapeutic Strategies, *Epilepsia* 51 (6) (2010) 1069–1077.
- [5] C.M. O'Dell, A. Das, Gt Wallace, S.K. Ray, N.L. Banik, Understanding the basic mechanisms underlying seizures in mesial temporal lobe epilepsy and possible therapeutic targets: a review, *J. Neurosci. Res.* 90 (5) (2012) 913–924.
- [6] K. Staley, Molecular mechanisms of epilepsy, *Nat. Neurosci.* 18 (3) (2015) 367–372.
- [7] S. Kovac, A.M. Domijan, M.C. Walker, A.Y. Abramov, Seizure activity results in calcium- and mitochondria-independent ROS production via NADPH and xanthine oxidase activation, *Cell Death Dis.* 5 (2014) e1442.
- [8] L.P. Liang, Y.S. Ho, M. Patel, Mitochondrial superoxide production in kainate-induced hippocampal damage, *Neuroscience* 101 (3) (2000) 563–570.
- [9] K. Ryan, L.P. Liang, C. Rivard, M. Patel, Temporal and spatial increase of reactive nitrogen species in the kainate model of temporal lobe epilepsy, *Neurobiol. Dis.* 64 (2014) 8–15.
- [10] S. Waldbaum, L.P. Liang, M. Patel, Persistent impairment of mitochondrial and tissue redox status during lithium-pilocarpine-induced epileptogenesis, *J. Neurochem.* 115 (5) (2010) 1172–1182.
- [11] S. Kovac, A.M. Domijan, M.C. Walker, A.Y. Abramov, Prolonged seizure activity impairs mitochondrial bioenergetics and induces cell death, *J. Cell Sci.* 125 (Pt 7) (2012) 1796–1806.
- [12] M. Patel, Mitochondrial dysfunction and oxidative stress: cause and consequence of epileptic seizures, *Free Radic. Biol. Med.* 37 (12) (2004) 1951–1962.
- [13] L.C. Abbott, H.H. Nejad, W.G. Botjje, A.S. Hassan, Glutathione levels in specific brain-regions of genetically epileptic (Tg/Tg) mice, *Brain Res. Bull.* 25 (4) (1990) 629–631.
- [14] P. Bhuyan, D.C. Patel, K.S. Wilcox, M. Patel, Oxidative stress in murine Theiler's virus-induced temporal lobe epilepsy, *Exp. Neurol.* 271 (2015) 329–334.
- [15] S.G. Mueller, A.H. Trabesinger, P. Boesiger, H.G. Wieser, Brain glutathione levels in patients with epilepsy measured by in vivo <sup>1</sup>H-MRS, *Neurology* 57 (8) (2001) 1422–1427.
- [16] R. Dringen, Metabolism and functions of glutathione in brain, *Prog Neurobiol* 62 (6) (2000) 649–671.
- [17] J.N. Cobley, M.L. Fiorello, D.M. Bailey, 13 reasons why the brain is susceptible to oxidative stress, *Redox Biol.* 15 (2018) 490–503.
- [18] K.F. Bell, B. Al-Mubarak, M.A. Martel, et al., Neuronal development is promoted by weakened intrinsic antioxidant defences due to epigenetic repression of Nrf2, *Nat. Commun.* 6 (2015) 7066.
- [19] P.S. Baxter, G.E. Hardingham, Adaptive regulation of the brain's antioxidant defences by neurons and astrocytes, *Free Radic. Biol. Med.* 100 (2016) 147–152.
- [20] C. Carrasco-Pozo, K.N. Tan, K. Borges, Sulforaphane is anticonvulsant and improves mitochondrial function, *J. Neurochem.* 135 (5) (2015) 932–942.
- [21] P.B. McElroy, A. Sri Hari, B.J. Day, M. Patel, Post-translational activation of glutamate cysteine ligase with dimeric caprol: a novel mechanism of inhibiting neuroinflammation in vitro, *J. Biol. Chem.* 292 (13) (2017) 5532–5545.
- [22] A. Pualetti, G. Terrone, T. Shekh-Ahmad, et al., Targeting oxidative stress improves disease outcomes in a rat model of acquired epilepsy, *Brain* 142 (7) (2019) e39.
- [23] L.M. Selwa, N-acetylcysteine therapy for Unverricht-Lundborg disease, *Neurology* 52 (2) (1999) 426–427.
- [24] T. Shekh-Ahmad, R. Eckel, S. Dayalan Naidu, et al., KEAP1 inhibition is neuroprotective and suppresses the development of epilepsy, *Brain* 141 (5) (2018) 1390–1403.
- [25] N. Singh, L. Saha, P. Kumari, et al., Effect of dimethyl fumarate on neuroinflammation and apoptosis in pentylenetetrazol kindling model in rats, *Brain Res. Bull.* 144 (2019) 233–245.
- [26] K.J.A. Davies, H.J. Forman, Does Bach 1 & c-Myc dependent redox dysregulation of Nrf2 & adaptive homeostasis decrease cancer risk in ageing? *Free Radic. Biol. Med.* 134 (2019) 708–714.
- [27] L. Zhou, H. Zhang, K.J.A. Davies, H.J. Forman, Aging-related decline in the induction of Nrf2-regulated antioxidant genes in human bronchial epithelial cells, *Redox Biol.* 14 (2018) 35–40.
- [28] S.J. Flora, V. Pachauri, Chelation in metal intoxication, *Int J Environ Res Public Health* 7 (7) (2010) 2745–2788.
- [29] D.K. Sandsmark, C. Pelletier, J.D. Weber, D.H. Gutmann, Mammalian target of rapamycin: master regulator of cell growth in the nervous system, *Histol. Histopathol.* 22 (8) (2007) 895–903.
- [30] D.D. Sarbassov, S.M. Ali, D.M. Sabatini, Growing roles for the mTOR pathway, *Curr. Opin. Cell Biol.* 17 (6) (2005) 596–603.
- [31] R.A. Saxton, D.M. Sabatini, mTOR signaling in growth, metabolism, and disease, *Cell* 168 (6) (2017) 960–976.
- [32] D.M. Talos, L.M. Jacobs, S. Gourmaud, et al., Mechanistic target of rapamycin complex 1 and 2 in human temporal lobe epilepsy, *Ann. Neurol.* 83 (2) (2018) 311–327.
- [33] P.B. Crino, Mechanistic target of rapamycin (mTOR) signaling in status epilepticus, *Epilepsy Behav.* 101 (Pt B) (2019), 106550.
- [34] P.B. McElroy, L.P. Liang, B.J. Day, M. Patel, Scavenging reactive oxygen species inhibits status epilepticus-induced neuroinflammation, *Exp. Neurol.* 298 (Pt A) (2017) 13–22.
- [35] L.H. Nguyen, T. Mahadeo, A. Bordey, mTOR hyperactivity levels influence the severity of epilepsy and associated neuropathology in an experimental model of tuberous sclerosis complex and focal cortical dysplasia, *J. Neurosci.* 39 (14) (2019) 2762–2773.
- [36] R.Y. Pun, I.J. Rolle, C.L. Lasarge, et al., Excessive activation of mTOR in postnatally generated granule cells is sufficient to cause epilepsy, *Neuron* 75 (6) (2012) 1022–1034.
- [37] A. Shima, N. Nitta, F. Suzuki, A.M. Laharie, K. Nozaki, A. Depaulis, Activation of mTOR signaling pathway is secondary to neuronal excitability in a mouse model of mesio-temporal lobe epilepsy, *Eur. J. Neurosci.* 41 (7) (2015) 976–988.
- [38] L.H. Zeng, N.R. Rensing, M. Wong, The mammalian target of rapamycin signaling pathway mediates epileptogenesis in a model of temporal lobe epilepsy, *J. Neurosci.* 29 (21) (2009) 6964–6972.
- [39] E. Russo, R. Citraro, G. Donato, et al., mTOR inhibition modulates epileptogenesis, seizures and depressive behavior in a genetic rat model of absence epilepsy, *Neuropharmacology* 69 (2013) 25–36.
- [40] M. Wong, Mammalian target of rapamycin (mTOR) activation in focal cortical dysplasia and related focal cortical malformations, *Exp. Neurol.* 244 (2013) 22–26.
- [41] M. Wong, mTOR strikes again: mTORC1 activation causes epilepsy independent of overt pathological changes, *Epilepsy Curr.* 14 (1) (2014) 41–43.
- [42] M. Wong, Commentary: mTOR inhibition suppresses established epilepsy in a mouse model of cortical dysplasia, *Epilepsia* 57 (9) (2016) 1349–1350.
- [43] F.J. Dumont, Q. Su, Mechanism of action of the immunosuppressant rapamycin, *Life Sci.* 58 (5) (1996) 373–395.
- [44] S.N. Sehgal, Rapamune (Sirolimus, rapamycin): an overview and mechanism of action, *Ther. Drug Monit.* 17 (6) (1995) 660–665.
- [45] P.S. Buckmaster, F.H. Lew, Rapamycin suppresses mossy fiber sprouting but not seizure frequency in a mouse model of temporal lobe epilepsy, *J. Neurosci.* 31 (6) (2011) 2337–2347.
- [46] M. Cardamone, D. Flanagan, D. Mowat, S.E. Kennedy, M. Chopra, J.A. Lawson, Mammalian target of rapamycin inhibitors for intractable epilepsy and subependymal giant cell astrocytomas in tuberous sclerosis complex, *J. Pediatr.* 164 (5) (2014) 1195–1200.
- [47] J. Muncy, I.J. Butler, M.K. Koenig, Rapamycin reduces seizure frequency in tuberous sclerosis complex, *J. Child Neurol.* 24 (4) (2009) 477.
- [48] A. Mingarelli, A. Vignoli, F. La Briola, et al., Dramatic relapse of seizures after everolimus withdrawal, *Eur. J. Paediatr. Neurol.* 22 (1) (2018) 203–206.
- [49] M. Li, L. Zhao, J. Liu, et al., Multi-mechanisms are involved in reactive oxygen species regulation of mTORC1 signaling, *Cell. Signal.* 22 (10) (2010) 1469–1476.
- [50] C.C. Dibble, W. Elis, S. Menon, et al., TBC1D7 is a third subunit of the TSC1-TSC2 complex upstream of mTORC1, *Mol Cell* 47 (4) (2012) 535–546.
- [51] H. Chong-Kopera, K. Inoki, Y. Li, et al., TSC1 stabilizes TSC2 by inhibiting the interaction between TSC2 and the HERC1 ubiquitin ligase, *J. Biol. Chem.* 281 (13) (2006) 8313–8316.
- [52] K. Inoki, Y. Li, T. Xu, K.L. Guan, Rheb GTPase is a direct target of TSC2 GAP activity and regulates mTOR signaling, *Genes Dev.* 17 (15) (2003) 1829–1834.
- [53] K. Yamagata, L.K. Sanders, W.E. Kaufmann, et al., rheb, a growth factor- and synaptic activity-regulated gene, encodes a novel Ras-related protein, *J. Biol. Chem.* 269 (23) (1994) 16333–16339.
- [54] U. Rehbein, M.T. Prentzell, M. Cadena Sandoval, et al., The TSC complex-mTORC1 Axis: from lysosomes to stress granules and back, *Front. Cell Dev. Biol.* 9 (2021), 751892.
- [55] H. Yang, X. Jiang, B. Li, et al., Mechanisms of mTORC1 activation by RHEB and inhibition by PRAS40, *Nature* 552 (7685) (2017) 368–373.
- [56] D.D. Sarbassov, D.M. Sabatini, Redox regulation of the nutrient-sensitive raptor-mTOR pathway and complex, *J. Biol. Chem.* 280 (47) (2005) 39505–39509.
- [57] S. Yoshida, S.K. Hong, T. Suzuki, et al., Redox regulates mammalian target of rapamycin complex 1 (mTORC1) activity by modulating the TSC1/TSC2-rheb GTPase pathway, *J. Biol. Chem.* 286 (37) (2011) 32651–32660.
- [58] M. Patel, B.J. Day, J.D. Crapo, I. Fridovich, J.O. McNamara, Requirement for superoxide in excitotoxic cell death, *Neuron* 16 (2) (1996) 345–355.

- [59] L.P. Liang, M. Patel, Seizure-induced changes in mitochondrial redox status, *Free Radic. Biol. Med.* 40 (2) (2006) 316–322.
- [60] B. Samborska, D.G. Roy, J.F. Rahbani, et al., Creatine transport and creatine kinase activity is required for CD8(+) T cell immunity, *Cell Rep.* 38 (9) (2022), 110446.
- [61] K. Nakashima, A. Ishida, AMP-Activated protein kinase activation suppresses protein synthesis and mTORC1 signaling in chick myotube cultures, *J. Poult. Sci.* 59 (1) (2022) 81–85.
- [62] J. Stagg, J. Sharkey, S. Pommey, et al., Antibodies targeted to TRAIL receptor-2 and ErbB-2 synergize in vivo and induce an antitumor immune response, *Proc Natl Acad Sci U S A* 105 (42) (2008) 16254–16259.
- [63] A. Anandhan, N. Nguyen, A. Syal, et al., NRF2 loss accentuates parkinsonian pathology and behavioral dysfunction in human alpha-synuclein overexpressing mice, *Aging Dis* 12 (4) (2021) 964–982.
- [64] Y. Huang, S. Wang, X. Meng, N. Chen, S. Li, Molecular cloning and characterization of sirtuin 1 and its potential regulation of lipid metabolism and antioxidant response in largemouth bass (*Micropterus salmoides*), *Front. Physiol.* 12 (2021), 726877.
- [65] K. Kumon, S.M. Afify, G. Hassan, et al., Differentiation of cancer stem cells into erythroblasts in the presence of CoCl<sub>2</sub>, *Sci. Rep.* 11 (1) (2021), 23977.
- [66] K. Benardais, I.M. Ornelas, M. Fauveau, et al., p70S6 kinase regulates oligodendrocyte differentiation and is active in remyelinating lesions, *Brain Commun* 4 (1) (2022), fca025.
- [67] L. Hinden, M. Ahmad, S. Hamad, et al., Opposite physiological and pathological mTORC1-mediated roles of the CB1 receptor in regulating renal tubular function, *Nat. Commun.* 13 (1) (2022) 1783.
- [68] Z. Wu, H. Huang, Q. Han, et al., SENP7 senses oxidative stress to sustain metabolic fitness and antitumor functions of CD8+ T cells, *J. Clin. Invest.* 132 (7) (2022).
- [69] P. Lopert, B.J. Day, M. Patel, Thioredoxin reductase deficiency potentiates oxidative stress, mitochondrial dysfunction and cell death in dopaminergic cells, *PLoS One* 7 (11) (2012), e50683.
- [70] E.S. Selen, M.J. Wolfgang, mTORC1 activation is not sufficient to suppress hepatic PPARalpha signaling or ketogenesis, *J. Biol. Chem.* 297 (1) (2021), 100884.
- [71] E.M. Mrozek, V. Bajaj, Y. Guo, I.A. Malinowska, J. Zhang, D.J. Kwiatkowski, Evaluation of Hsp 90 and mTOR inhibitors as potential drugs for the treatment of TSC1/TSC2 deficient cancer, *PLoS One* 16 (4) (2021), e0248380.
- [72] M.T. Prentzell, U. Rehbein, M. Cadena Sandoval, et al., G3BPs tether the TSC complex to lysosomes and suppress mTORC1 signaling, *Cell* 184 (3) (2021) 655–674, e627.
- [73] F. Choo, I. Odintsov, K. Nusser, et al., Functional impact and targetability of PI3KCA, GNAS, and PTEN mutations in a spindle cell rhabdomyosarcoma with MYOD1 L122R mutation, *Cold Spring Harb Mol Case Stud* 8 (1) (2022).
- [74] N.C. Gassen, J. Papies, T. Bajaj, et al., SARS-CoV-2-mediated dysregulation of metabolism and autophagy uncovers host-targeting antivirals, *Nat. Commun.* 12 (1) (2021) 3818.
- [75] C.U. Oeing, S. Jun, S. Mishra, et al., mTORC1-Regulated metabolism controlled by TSC2 limits cardiac reperfusion injury, *Circ. Res.* 128 (5) (2021) 639–651.
- [76] S. Wei, M. Dai, C. Zhang, et al., KIF2C: a novel link between Wnt/beta-catenin and mTORC1 signaling in the pathogenesis of hepatocellular carcinoma, *Protein Cell* 12 (10) (2021) 788–809.
- [77] C. Demetriades, M. Plescher, A.A. Teleman, Lysosomal recruitment of TSC2 is a universal response to cellular stress, *Nat. Commun.* 7 (2016), 10662.
- [78] A. Najafov, H.S. Luu, A.K. Mookhtiar, et al., RIPK1 promotes energy sensing by the mTORC1 pathway, *Mol Cell* 81 (2) (2021) 370–385 e377.
- [79] M. Westerfield, *The Zebrafish Book: a Guide for the Laboratory Use of Zebrafish*, 2000. <http://zfinfo.org/zfinfo/zfbok/zfbk.html>.
- [80] M.G. Kumar, S. Rowley, R. Fulton, M.T. Dinday, S.C. Baraban, M. Patel, Altered glycolysis and mitochondrial respiration in a zebrafish model of Dravet syndrome, *eNeuro* 3 (2) (2016).
- [81] S.C. Baraban, M.T. Dinday, G.A. Hortopan, Drug screening in Scn1a zebrafish mutant identifies clemizole as a potential Dravet syndrome treatment, *Nat. Commun.* 4 (2013) 2410.
- [82] A. Griffin, K.R. Hamling, K. Knupp, S. Hong, L.P. Lee, S.C. Baraban, Clemizole and modulators of serotonin signalling suppress seizures in Dravet syndrome, *Brain* 140 (3) (2017) 669–683.
- [83] A.E. Novak, M.C. Jost, Y. Lu, A.D. Taylor, H.H. Zakon, A.B. Ribera, Gene duplications and evolution of vertebrate voltage-gated sodium channels, *J. Mol. Evol.* 63 (2) (2006) 208–221.
- [84] Noldus DanioVision. <https://www.noldus.com/applications/compound-screening>
- [85] S.C. Baraban, M.T. Dinday, P.A. Castro, S. Chege, S. Guyenet, M.R. Taylor, A large-scale mutagenesis screen to identify seizure-resistant zebrafish, *Epilepsia* 48 (6) (2007) 1151–1157.
- [86] R. Banerji, C. Huynh, F. Figueroa, M.T. Dinday, S.C. Baraban, M. Patel, Enhancing glucose metabolism via gluconeogenesis is therapeutic in a zebrafish model of Dravet syndrome, *Brain Commun* 3 (1) (2021).
- [87] D.L. Tomasello, H. Sive, Noninvasive multielectrode array for brain and spinal cord local field potential recordings from live zebrafish larvae, *Zebrafish* 17 (4) (2020) 271–277.
- [88] M. Meyer, S.C. Dhamne, C.M. LaCoursiere, D. Tambunan, A. Poduri, A. Rotenberg, Correction: microarray noninvasive neuronal seizure recordings from intact larval zebrafish, *PLoS One* 11 (7) (2016), e0159472.
- [89] M. Meyer, S.C. Dhamne, C.M. LaCoursiere, D. Tambunan, A. Poduri, A. Rotenberg, Microarray noninvasive neuronal seizure recordings from intact larval zebrafish, *PLoS One* 11 (6) (2016), e0156498.
- [90] D. Choquet, H. Korn, Mechanism of 4-aminopyridine action on voltage-gated potassium channels in lymphocytes, *J. Gen. Physiol.* 99 (2) (1992) 217–240.
- [91] Y. Berdichevsky, A.M. Dryer, Y. Saponjian, et al., PI3K-Akt signaling activates mTOR-mediated epileptogenesis in organotypic hippocampal culture model of post-traumatic epilepsy, *J. Neurosci.* 33 (21) (2013) 9056–9067.
- [92] X. Huang, H. Zhang, J. Yang, et al., Pharmacological inhibition of the mammalian target of rapamycin pathway suppresses acquired epilepsy, *Neurobiol. Dis.* 40 (1) (2010) 193–199.
- [93] J.L. Griffith, M. Wong, The mTOR pathway in treatment of epilepsy: a clinical update, *Future Neurol.* 13 (2) (2018) 49–58.
- [94] J. Liu, C. Reeves, Z. Michalak, et al., Evidence for mTOR pathway activation in a spectrum of epilepsy-associated pathologies, *Acta Neuropathol Commun* 2 (2014) 71.
- [95] A.M. Heberle, M.T. Prentzell, K. van Eunen, B.M. Bakker, S.N. Grellescheid, K. Thedieck, Molecular mechanisms of mTOR regulation by stress, *Mol Cell Oncol* 2 (2) (2015), e970489.
- [96] D. Zhao, J. Yang, L. Yang, Insights for oxidative stress and mTOR signaling in myocardial ischemia/reperfusion injury under diabetes, *Oxid. Med. Cell. Longev.* (2017), 6437467, 2017.
- [97] L. Chen, B. Xu, L. Liu, et al., Cadmium induction of reactive oxygen species activates the mTOR pathway, leading to neuronal cell death, *Free Radic. Biol. Med.* 50 (5) (2011) 624–632.
- [98] W. He, J. Chen, Y.Y. Wang, et al., Erratum to "Sirolimus improves seizure control in pediatric patients with tuberous sclerosis: a prospective cohort study", *Seizure: Eur. J. Epilepsy* 79 (2020) 20–26. [Seizure. 2020;81:342.](https://doi.org/10.1016/j.seizure.2020.08.034)
- [99] W. He, J. Chen, Y.Y. Wang, et al., Sirolimus improves seizure control in pediatric patients with tuberous sclerosis: a prospective cohort study, *Seizure* 79 (2020) 20–26.
- [100] M. Wong, Rapamycin for treatment of epilepsy: antiseizure, antiepileptogenic, both, or neither? *Epilepsy Curr.* 11 (2) (2011) 66–68.
- [101] O.W. Griffith, Mechanism of action, metabolism, and toxicity of buthionine sulfoximine and its higher homologs, potent inhibitors of glutathione synthesis, *J. Biol. Chem.* 257 (22) (1982) 13704–13712.
- [102] A. Meister, Glutathione biosynthesis and its inhibition, *Methods Enzymol.* 252 (1995) 26–30.
- [103] D.B. Peruchetti, J. Cheng, C. Caruso-Neves, W.B. Guggino, Mis-regulation of mammalian target of rapamycin (mTOR) complexes induced by albuminuria in proximal tubules, *J. Biol. Chem.* 289 (24) (2014) 16790–16801.
- [104] S. Sengupta, T.R. Peterson, D.M. Sabatini, Regulation of the mTOR complex 1 pathway by nutrients, growth factors, and stress, *Mol Cell* 40 (2) (2010) 310–322.
- [105] T.H. Truong, K.S. Carroll, Redox regulation of protein kinases, *Crit. Rev. Biochem. Mol. Biol.* 48 (4) (2013) 332–356.
- [106] H.J. Forman, H. Zhang, A. Rinna, Glutathione: overview of its protective roles, measurement, and biosynthesis, *Mol Aspects Med* 30 (1–2) (2009) 1–12.
- [107] P. Ghezzi, Regulation of protein function by glutathionylation, *Free Radic. Res.* 39 (6) (2005) 573–580.
- [108] S. Biswas, A.S. Chida, I. Rahman, Redox modifications of protein-thiols: emerging roles in cell signaling, *Biochem. Pharmacol.* 71 (5) (2006) 551–564.
- [109] A.J. Cooper, J.T. Pinto, P.S. Callery, Reversible and irreversible protein glutathionylation: biological and clinical aspects, *Expert Opin Drug Metab Toxicol* 7 (7) (2011) 891–910.
- [110] J. Huang, B.D. Manning, The TSC1-TSC2 complex: a molecular switchboard controlling cell growth, *Biochem. J.* 412 (2) (2008) 179–190.
- [111] I. Fanelus, R.R. Desrosiers, Reactive oxygen species generated by thiol-modifying phenylarsine oxide stimulate the expression of protein L-isoaspartyl methyltransferase, *Biochem. Biophys. Res. Commun.* 371 (2) (2008) 203–208.
- [112] R.K. Srivastava, C. Li, Z. Weng, et al., Defining cutaneous molecular pathobiology of arsenicals using phenylarsine oxide as a prototype, *Sci. Rep.* 6 (2016), 34865.
- [113] W.W. Cleland, Dithiothreitol, a new protective reagent for sh groups, *Biochemistry* 3 (1964) 480–482.
- [114] N. Zepeta-Flores, M. Valverde, A. Lopez-Saavedra, E. Rojas, Glutathione depletion triggers actin cytoskeleton changes via actin-binding proteins, *Genet. Mol. Biol.* 41 (2) (2018) 475–487.
- [115] A. Banerjee, M.A. Jordan, R.F. Luduena, Interaction of reduced glutathione with bovine brain tubulin, *Biochem. Biophys. Res. Commun.* 128 (2) (1985) 506–512.
- [116] J. Guo, H.S. Kim, R. Asmis, R.F. Luduena, Interactions of beta tubulin isoforms with glutathione in differentiated neuroblastoma cells subject to oxidative stress, *Cytoskeleton (Hoboken)* 75 (7) (2018) 283–289.
- [117] Y.M. Go, D.P. Jones, Thioredoxin redox western analysis, *Curr Protoc Toxicol* (2009) (Chapter 17):Unit17 12.
- [118] D.D. Sarbassov, D.M. Sabatini, Redox regulation of the nutrient-sensitive rapamycin pathway and complex, *J. Biol. Chem.* 280 (47) (2005) 39505–39509.
- [119] C. Lange, F. Rost, A. Machate, et al., Single cell sequencing of radial glia progeny reveals the diversity of newborn neurons in the adult zebrafish brain, *Development* 147 (1) (2020).
- [120] B. Raj, D.E. Wagner, A. McKenna, et al., Simultaneous single-cell profiling of lineages and cell types in the vertebrate brain, *Nat. Biotechnol.* 36 (5) (2018) 442–450.
- [121] D.G.C. Hildebrand, M. Cicconet, R.M. Torres, et al., Whole-brain serial-section electron microscopy in larval zebrafish, *Nature* 545 (7654) (2017) 345–349.
- [122] M. Kunst, E. Laurell, N. Mokayes, et al., A cellular-resolution atlas of the larval zebrafish brain, *Neuron* 103 (1) (2019) 21–38, e25.

- [123] A. Rastogi, C.W. Clark, S.M. Conlin, S.E. Brown, A.R. Timme-Laragy, Mapping glutathione utilization in the developing zebrafish (*Danio rerio*) embryo, *Redox Biol.* 26 (2019), 101235.
- [124] J. Liu, S.C. Baraban, Network properties revealed during multi-scale calcium imaging of seizure activity in zebrafish, *eNeuro* 6 (1) (2019).
- [125] T. Afrikanova, A.S. Serruys, O.E. Buenafe, et al., Validation of the zebrafish pentylenetetrazol seizure model: locomotor versus electrographic responses to antiepileptic drugs, *PLoS One* 8 (1) (2013), e54166.
- [126] S.C. Baraban, M.R. Taylor, P.A. Castro, H. Baier, Pentylenetetrazole induced changes in zebrafish behavior, neural activity and c-Fos expression, *Neuroscience* 131 (3) (2005) 759–768.
- [127] P. Uma Devi, K.K. Pillai, D. Vohora, Modulation of pentylenetetrazole-induced seizures and oxidative stress parameters by sodium valproate in the absence and presence of N-acetylcysteine, *Fundam. Clin. Pharmacol.* 20 (3) (2006) 247–253.
- [128] S. Baxendale, C.J. Holdsworth, P.L. Meza Santoscoy, et al., Identification of compounds with anti-convulsant properties in a zebrafish model of epileptic seizures, *Dis Model Mech* 5 (6) (2012) 773–784.
- [129] P.C. Milder, A.S. Zybura, T.R. Cummins, J.A. Marrs, Neural activity correlates with behavior effects of anti-seizure drugs efficacy using the zebrafish pentylenetetrazol seizure model, *Front. Pharmacol.* 13 (2022), 836573.
- [130] P.J. Schoonheim, A.B. Arrenberg, F. Del Bene, H. Baier, Optogenetic localization and genetic perturbation of saccade-generating neurons in zebrafish, *J. Neurosci.* 30 (20) (2010) 7111–7120.
- [131] C. Dravet, The core Dravet syndrome phenotype, *Epilepsia* 52 (s2) (2011) 3–9.
- [132] C. Dravet, M. Bureau, H. Oguni, Y. Fukuyama, O. Cokar, Severe myoclonic epilepsy in infancy (Dravet syndrome), *Epileptic syndromes in infancy, childhood and adolescence* 4 (2005) 89–113.
- [133] A. Massarsky, J.S. Kozal, R.T. Di Giulio, Glutathione and zebrafish: old assays to address a current issue, *Chemosphere* 168 (2017) 707–715.
- [134] M.L. Buck, H.P. Goodkin, Stiripentol: a novel antiseizure medication for the management of Dravet syndrome, *Ann. Pharmacother.* 53 (11) (2019) 1136–1144.
- [135] J.E. Frampton, Stiripentol: a review in Dravet syndrome, *Drugs* 79 (16) (2019) 1785–1796.
- [136] S.C. Baraban, M.T. Dinday, G.A. Hortopan, Drug screening in *Scn1a* zebrafish mutant identifies clemizole as a potential Dravet syndrome treatment, *Nat. Commun.* 4 (2013).
- [137] A. Destexhe, C. Bédard, Local field potentials (LFP), in: D. Jaeger, R. Jung (Eds.), *Encyclopedia of Computational Neuroscience*, Springer New York, New York, NY, 2013, pp. 1–11.
- [138] D. Golomb, J. Rinzel, Dynamics of globally coupled inhibitory neurons with heterogeneity, *Phys Rev E Stat Phys Plasmas Fluids Relat Interdiscip Topics* 48 (6) (1993) 4810–4814.
- [139] D. Hansel, G. Mato, C. Meunier, Clustering and slow switching in globally coupled phase oscillators, *Phys Rev E Stat Phys Plasmas Fluids Relat Interdiscip Topics* 48 (5) (1993) 3470–3477.
- [140] Ginzburg II, H. Sompolinsky, Theory of correlations in stochastic neural networks, *Phys Rev E Stat Phys Plasmas Fluids Relat Interdiscip Topics* 50 (4) (1994) 3171–3191.
- [141] S. Desagher, J. Glowinski, J. Premont, Astrocytes protect neurons from hydrogen peroxide toxicity, *J. Neurosci.* 16 (8) (1996) 2553–2562.
- [142] X. Ren, L. Zou, X. Zhang, et al., Redox signaling mediated by thioredoxin and glutathione systems in the central nervous system, *Antioxidants Redox Signal.* 27 (13) (2017) 989–1010.
- [143] P.M. Sinet, R.E. Heikkilä, G. Cohen, Hydrogen peroxide production by rat brain in vivo, *J. Neurochem.* 34 (6) (1980) 1421–1428.
- [144] J.N. Pearson, M. Patel, The role of oxidative stress in organophosphate and nerve agent toxicity, *Ann. N. Y. Acad. Sci.* 1378 (1) (2016) 17–24.
- [145] J.B. Milder, L.P. Liang, M. Patel, Acute oxidative stress and systemic Nrf2 activation by the ketogenic diet, *Neurobiol. Dis.* 40 (1) (2010) 238–244.
- [146] A.J. Meade, B.P. Meloni, F.L. Mastaglia, P.M. Watt, N.W. Knuckey, AP-1 inhibitory peptides attenuate in vitro cortical neuronal cell death induced by kainic acid, *Brain Res.* 1360 (2010) 8–16.
- [147] H. Heuzeroth, M. Wawra, P. Fidzinski, R. Dag, M. Holtkamp, The 4-aminopyridine model of acute seizures in vitro elucidates efficacy of new antiepileptic drugs, *Front. Neurosci.* 13 (2019) 677.
- [148] M. Levesque, P. Salami, C. Behr, M. Avoli, Temporal lobe epileptiform activity following systemic administration of 4-aminopyridine in rats, *Epilepsia* 54 (4) (2013) 596–604.
- [149] J. Frago-Veloz, L. Massieu, R. Alvarado, R. Tapia, Seizures and wet-dog shakes induced by 4-aminopyridine, and their potentiation by nifedipine, *Eur. J. Pharmacol.* 178 (3) (1990) 275–284.
- [150] A. Mihaly, K. Bencsik, T. Solymosi, Naltrexone potentiates 4-aminopyridine seizures in the rat, *J. Neural Transm. Gen. Sect.* 79 (1–2) (1990) 59–67.
- [151] S. Yamaguchi, M.A. Rogawski, Effects of anticonvulsant drugs on 4-aminopyridine-induced seizures in mice, *Epilepsy Res.* 11 (1) (1992) 9–16.
- [152] H. Pasantes-Morales, M.E. Arzate, Effect of taurine on seizures induced by 4-aminopyridine, *J. Neurosci. Res.* 6 (4) (1981) 465–474.
- [153] L. Xu, N. Rensing, X.F. Yang, et al., Leptin inhibits 4-aminopyridine- and pentylenetetrazole-induced seizures and AMPAR-mediated synaptic transmission in rodents, *J. Clin. Invest.* 118 (1) (2008) 272–280.
- [154] E.D. Martin, M.A. Pozo, Valproate suppresses status epilepticus induced by 4-aminopyridine in CA1 hippocampus region, *Epilepsia* 44 (11) (2003) 1375–1379.
- [155] C. Bruckner, U. Heinemann, Effects of standard anticonvulsant drugs on different patterns of epileptiform discharges induced by 4-aminopyridine in combined entorhinal cortex-hippocampal slices, *Brain Res.* 859 (1) (2000) 15–20.
- [156] T.A. Pickett, R. Enns, Atypical presentation of 4-aminopyridine overdose, *Ann. Emerg. Med.* 27 (3) (1996) 382–385.
- [157] C.M. Stork, R.S. Hoffman, Characterization of 4-aminopyridine in overdose, *J. Toxicol. Clin. Toxicol.* 32 (5) (1994) 583–587.
- [158] J. Folbergrova, P. Jesina, H. Kubova, R. Druga, J. Otahal, Status epilepticus in immature rats is associated with oxidative stress and mitochondrial dysfunction, *Front. Cell. Neurosci.* 10 (2016) 136.
- [159] J.G. Luft, L. Steffens, A.M. Moras, et al., Rosmarinic acid improves oxidative stress parameters and mitochondrial respiratory chain activity following 4-aminopyridine and picrotoxin-induced seizure in mice, *Naunyn-Schmiedeberg's Arch. Pharmacol.* 392 (11) (2019) 1347–1358.
- [160] C. Oner, E. Colak, D.T. Gosan, Potassium channel inhibitors induce oxidative stress in breast cancer cells, *Asian Biomed.* 11 (4) (2017) 323–330.
- [161] L.A. Kasatkina, 4-capital A, Cycliciminopyridine sequesters intracellular Ca(2+) which triggers exocytosis in excitable and non-excitable cells, *Sci. Rep.* 6 (2016), 34749.
- [162] A. Morales-Villagran, R. Tapia, Preferential stimulation of glutamate release by 4-aminopyridine in rat striatum in vivo, *Neurochem. Int.* 28 (1) (1996) 35–40.
- [163] P.A. Rutecki, F.J. Lebeda, D. Johnston, 4-Aminopyridine produces epileptiform activity in hippocampus and enhances synaptic excitation and inhibition, *J. Neurophysiol.* 57 (6) (1987) 1911–1924.
- [164] H. Slevin, J.E. Gibbs, S. Heales, M. Thom, H.R. Cock, Depletion of reduced glutathione precedes inactivation of mitochondrial enzymes following limbic status epilepticus in the rat hippocampus, *Neurochem. Int.* 48 (2) (2006) 75–82.
- [165] T.W. Sedlak, L.G. Nucifora, M. Koga, et al., Sulforaphane augments glutathione and influences brain metabolites in human subjects: a clinical pilot study, *Mol. Neuropsychiatry* 3 (4) (2018) 214–222.
- [166] R.W. Hurd, B.J. Wilder, W.R. Helveston, B.M. Uthman, Treatment of four siblings with progressive myoclonus epilepsy of the Unverricht-Lundborg type with N-acetylcysteine, *Neurology* 47 (5) (1996) 1264–1268.
- [167] T. Kramer, T. Grob, L. Menzel, et al., Dimethyl fumarate treatment after traumatic brain injury prevents depletion of antioxidative brain glutathione and confers neuroprotection, *J. Neurochem.* 143 (5) (2017) 523–533.
- [168] S.G. Jarrett, J.B. Milder, L.P. Liang, M. Patel, The ketogenic diet increases mitochondrial glutathione levels, *J. Neurochem.* 106 (3) (2008) 1044–1051.
- [169] J. Milder, M. Patel, Modulation of oxidative stress and mitochondrial function by the ketogenic diet, *Epilepsy Res.* 100 (3) (2012) 295–303.
- [170] A. Napolitano, D. Longo, M. Lucignani, et al., The ketogenic diet increases in vivo glutathione levels in patients with epilepsy, *Metabolites* 10 (12) (2020).
- [171] M. Laplante, D.M. Sabatini, mTOR signaling at a glance, *J. Cell Sci.* 122 (Pt 20) (2009) 3589–3594.
- [172] X.Z. Li, X.H. Yan, Sensors for the mTORC1 pathway regulated by amino acids, *J. Zhejiang Univ. - Sci. B* 20 (9) (2019) 699–712.
- [173] C. Tokunaga, K. Yoshino, K. Yonezawa, mTOR integrates amino acid- and energy-sensing pathways, *Biochem. Biophys. Res. Commun.* 313 (2) (2004) 443–446.
- [174] C.L. Lasage, S.C. Danzer, Mechanisms regulating neuronal excitability and seizure development following mTOR pathway hyperactivation, *Front. Mol. Neurosci.* 7 (2014) 18.
- [175] G. Leprieux, B. Rotblat, How does mTOR sense glucose starvation? AMPK is the usual suspect, *Cell Death Discov* 6 (2020) 27.
- [176] L.H. Nguyen, A.L. Brewster, M.E. Clark, et al., mTOR inhibition suppresses established epilepsy in a mouse model of cortical dysplasia, *Epilepsia* 56 (4) (2015) 636–646.
- [177] M. Baybis, L. Yu, A. Lee, et al., Activation of the mTOR Cascade Distinguishes Cortical Tubers from Focal Cortical Dysplasia, 2004. Paper presented at: EPILEPSIA.
- [178] P.B. Crino, mTOR: a pathogenic signaling pathway in developmental brain malformations, *Trends Mol. Med.* 17 (12) (2011) 734–742.
- [179] M.C. Ljungberg, M.B. Bhattacharjee, Y. Lu, et al., Activation of mammalian target of rapamycin in cytomegalic neurons of human cortical dysplasia, *Ann. Neurol.* 60 (4) (2006) 420–429.
- [180] S.S. McDaniel, N.R. Rensing, L.L. Thio, K.A. Yamada, M. Wong, The ketogenic diet inhibits the mammalian target of rapamycin (mTOR) pathway, *Epilepsia* 52 (3) (2011) e7–e11.
- [181] D.R. Ziegler, L.C. Ribeiro, M. Hagenn, et al., Ketogenic diet increases glutathione peroxidase activity in rat hippocampus, *Neurochem. Res.* 28 (12) (2003) 1793–1797.
- [182] Z.W. Lai, R. Hanczko, E. Bonilla, et al., N-acetylcysteine reduces disease activity by blocking mammalian target of rapamycin in T cells from systemic lupus erythematosus patients: a randomized, double-blind, placebo-controlled trial, *Arthritis Rheum.* 64 (9) (2012) 2937–2946.
- [183] S. Sudarshan, M. Kumar, P. Kaur, et al., Decoding of novel missense TSC2 gene variants using in-silico methods, *BMC Med. Genet.* 20 (1) (2019) 164.
- [184] D.P. Jones, Redox potential of GSH/GSSG couple: assay and biological significance, *Methods Enzymol.* 348 (2002) 93–112.
- [185] F.Q. Schafer, G.R. Buettner, Redox environment of the cell as viewed through the redox state of the glutathione disulfide/glutathione couple, *Free Radic. Biol. Med.* 30 (11) (2001) 1191–1212.
- [186] K. Aquilano, S. Baldelli, M.R. Ciriolo, Glutathione: new roles in redox signaling for an old antioxidant, *Front. Pharmacol.* 5 (2014) 196.
- [187] J.S. Armstrong, K.K. Steinauer, B. Hornung, et al., Role of glutathione depletion and reactive oxygen species generation in apoptotic signaling in a human B lymphoma cell line, *Cell Death Differ.* 9 (3) (2002) 252–263.
- [188] D.R.W. Burrows, E. Samarut, J. Liu, et al., Imaging epilepsy in larval zebrafish, *Eur. J. Paediatr. Neurol.* 24 (2020) 70–80.

- [189] J. Sourbron, M. Partoens, C. Scheldeman, Y. Zhang, L. Lagae, P. de Witte, Drug repurposing for Dravet syndrome in *scn1Lab(-/-)* mutant zebrafish, *Epilepsia* 60 (2) (2019) e8–e13.
- [190] A.R. Timme-Laragy, J.V. Goldstone, B.R. Imhoff, J.J. Stegeman, M.E. Hahn, J. M. Hansen, Glutathione redox dynamics and expression of glutathione-related genes in the developing embryo, *Free Radic. Biol. Med.* 65 (2013) 89–101.
- [191] B.K.M. Choo, U.P. Kundap, S.M.M. Faudzi, F. Abas, M.F. Shaikh, E. Samarut, Identification of curcumin analogues with anti-seizure potential in vivo using chemical and genetic zebrafish larva seizure models, *Biomed. Pharmacother.* 142 (2021), 112035.
- [192] M. Jin, Q. He, S. Zhang, Y. Cui, L. Han, K. Liu, Gastrodin suppresses pentylenetetrazole-induced seizures progression by modulating oxidative stress in zebrafish, *Neurochem. Res.* 43 (4) (2018) 904–917.
- [193] S. Zaeri, M. Emamghoreishi, Acute and chronic effects of N-acetylcysteine on pentylenetetrazole-induced seizure and neuromuscular coordination in mice, *Iran. J. Med. Sci.* 40 (2) (2015) 118–124.
- [194] K.J. Bough, R. Valiyil, F.T. Han, D.A. Eagles, Seizure resistance is dependent upon age and calorie restriction in rats fed a ketogenic diet, *Epilepsy Res.* 35 (1) (1999) 21–28.
- [195] E. Raffo, J. Francois, A. Ferrandon, E. Koning, A. Nehlig, Calorie-restricted ketogenic diet increases thresholds to all patterns of pentylenetetrazol-induced seizures: critical importance of electroclinical assessment, *Epilepsia* 49 (2) (2008) 320–328.
- [196] A. Arzimanoglou, Dravet syndrome: from electroclinical characteristics to molecular biology, *Epilepsia* 50 (s8) (2009) 3–9.
- [197] C. Dravet, Dravet syndrome history, *Dev. Med. Child Neurol.* 53 (s2) (2011) 1–6.
- [198] A. Strzelczyk, S. Schubert-Bast, Therapeutic advances in Dravet syndrome: a targeted literature review, *Expert Rev. Neurother.* 20 (10) (2020) 1065–1079.
- [199] S.C. Baraban, Forebrain electrophysiological recording in larval zebrafish, *J. Vis. Exp.* 71 (2013).
- [200] R.H. Caraballo, R.O. Cersosimo, D. Sakr, A. Cresta, N. Escobal, N. Fejerman, Ketogenic diet in patients with Dravet syndrome, *Epilepsia* 46 (9) (2005) 1539–1544.
- [201] L. Laux, R. Blackford, The ketogenic diet in Dravet syndrome, *J. Child Neurol.* 28 (8) (2013) 1041–1044.
- [202] Y.Q. Wang, Z.X. Fang, Y.W. Zhang, L.L. Xie, L. Jiang, Efficacy of the ketogenic diet in patients with Dravet syndrome: a meta-analysis, *Seizure* 81 (2020) 36–42.
- [203] A. Strzelczyk, S. Schubert-Bast, A practical Guide to the treatment of Dravet syndrome with anti-seizure medication, *CNS Drugs* 36 (3) (2022) 217–237.
- [204] S.A. Masino, J.M. Rho, Mechanisms of ketogenic diet action, in: J.L. Noebels, M. Avoli, M.A. Rogawski, R.W. Olsen, A.V. Delgado-Escueta (Eds.), *Jasper's Basic Mechanisms of the Epilepsies*, 2012, 4th ed. Bethesda (MD).